



SAPIENZA
Università di Roma
Facoltà di Farmacia e Medicina

Ph.D. in
MORPHOGENESIS AND TISSUE ENGINEERING

XXXII Ciclo
(A.A.2018-2019)

***c-MET activated pathways and their implication in TGCTs
oncogenesis***

Ph.D. Student
Erica Leonetti

Tutors
Prof. Angiolina Catizone
Prof. Giulia Ricci

Coordinator
Prof. Antonio Musarò

Erica Leonetti

A mamma e papà,
fonte di amore costante.
Ai miei nonni meravigliosi,
il cui affetto è scolpito indelebile nel mio cuore,
con la speranza di averli resi orgogliosi
ovunque essi siano.
A zia Emma,
che ha creduto in me e mi ha amata sin dal principio.
A Francesco,
che mi ha tenuta per mano
in ogni tappa del mio percorso.

A me stessa,
per aver sempre trovato la
forza di rialzarmi.

Erica Leonetti

INDEX

1. Summary 9

 1.1 Biological issue 9

 1.2 Results obtained..... 9

 1.3 Conclusions 10

2. Introduction 11

 2.1 Germ Cell Tumours (GCTs) 11

 2.1.1 Classification..... 11

 2.1.2 Testicular Germ Cell Tumours (Type II) 11

 2.1.3 Origin of Type II TGCTs 12

 2.1.4 Risk Factor 14

 2.1.5 Chemio- and radio- resistance acquisition 18

 2.1.6 Cell lines and models..... 20

 2.2 HGF/c-MET system 20

 2.2.1 Hepatocyte Growth Factor (HGF)..... 20

 2.2.2 Mesenchymal Epithelial Transition (c-MET)..... 21

 2.2.3 HGF/c-MET signal transduction..... 23

 2.2.4 HGF/c-MET in testis..... 26

 2.2.5 HGF/c-MET de-regulation in human cancer 27

 2.3 c-MET in TGCTs..... 30

 2.3.2 My previous work..... 31

3. Aims..... 33

4. Results 35

 4.1 c-MET modulates the migration of NT2D1 cells induced by HGF. 35

4.1.1 NT2D1 chemo-attraction is specifically driven by c-MET	35
4.1.2a c-MET modulates the collective migration of NT2D1 cells induced by HGF.....	36
4.2 c-Src is involved in HGF-dependent NT2D1 responses	41
4.2.1 Src inhibitor-1 does not affect cell viability	41
4.2.2 c-Src is involved in HGF-dependent NT2D1 proliferation	42
4.2.3 c-Src is specifically involved in HGF-dependent NT2D1 chemo-attraction	44
4.2.4 c-Src is involved in HGF-induced collective migration	45
4.2.5 c-Src is involved in HGF-dependent cells invasion	47
4.2.6 Phospho-c-Src detection after HGF administration	49
4.2.7 Immunofluorescence analysis of the active form of c-Src (phospho Tyr 416).....	50
4.3. PI3K/AKT involvement in NT2D1 cellular responses.....	52
4.3.1 PI3K/AKT is active in NT2D1 cells and LY294002 does not affect cell viability	52
4.3.2 HGF-dependent NT2D1 proliferation is dependent on PI3K/AKT	53
4.3.3 PI3/AKT pathway is involved in HGF-dependent NT2D1 migration	54
4.3.4 PI3K/AKT pathway is involved in HGF-induced collective migration	56
4.3.5 PI3K is involved in HGF-dependent cells invasion.....	58
4.3.6 HGF induced NT2D1morphological modification through PI3K/AKT	59
4.4 Link between c-Src and PI3K/AKT	62

4.4.1 Relation between PI3K/AKT and c-Src proteins	62
4.4.2 Cytoskeletal remodeling HGF-dependent in NT2D1 cells	63
4.5 HGF expression in TGCTs biopsies.....	67
4.5.1 HGF distribution pattern in TGCT histological samples.....	67
Discussion.....	71
5. Materials and Methods.....	77
5.1 Cell Culture.....	77
5.2 Cell Proliferation Assay.....	77
5.3 Cell Cycle FACS Analysis.....	78
5.4. Cell Death Assay	78
5.5 Chemotaxis Assay	78
5.6 Wound-healing Assay (Collective Migration Assay)	79
5.7 Matrigel Invasion Assay.....	80
5.8 Immunofluorescence Analyses and actin staining	81
5.9 Western Blot Analyses	82
5.10 Scanning Electron Microscopy	83
5.11 Immunohistochemical Analyses.....	83
5.12 Statistical Analyses	84
6. List of abbreviations	85
7. References.....	87
List of publications	99
Congress communications	101
Acknowledgments:.....	105

Erica Leonetti

1. Summary

1.1 Biological issue

Type II Testicular Germ Cell Tumors (TGCTs) are a group of pathologies whose incidence has increased in the recent years in young men between 15 and 39 years old. Their pathogenesis is not yet entirely clear, but the survival rate in patients suffering from TGCTs is good. In fact, about 90-95% of these patients recover. However, the increased incidence of TGCTs and the fact that the onset of these tumours typically arises in young people make necessary the development of new drugs and therapies for the 5-10% of patients who develop drug resistance, radio-resistance or long-term toxicity. HGF/c-MET is a very complex system, which is essential during embryogenesis and necessary for the maintenance of tissue homeostasis. Moreover, it is well known that this system results de-regulated in the onset and progression of several human cancers. My group recently demonstrated the differential expression of c-MET receptor in Type II TGCT representative cell lines. Non-seminoma cells result in higher biological responses induced by HGF with respect to other cell lines analysed. c-MET expression was also observed in biopsies derived from patients affected by all type II TGCTs. In this thesis we investigate the various HGF/c-MET activated pathways and the role of these proteins in non-seminoma cell line responses in a HGF-dependent way. Moreover, HGF immunoreactivity was also evaluated in patients affected by TGCTs in order to have a better understanding on the TGCTs pathogenesis.

1.2 Results obtained

The obtained results demonstrated that c-Src and PI3K/AKT pathways are involved in the following HGF-dependent biological responses in non-seminoma cells: proliferation, migration and invasion increase. c-Src is constitutively active in NT2D1 cells and is involved also in proliferation, invasion and collective migration in an HGF-independent manner. On the other hand, also PI3K/AKT is involved in the endogenous NT2D1 collective migration and invasion.

HGF is expressed in biopsies derived from SE and EC. In particular, EC samples exhibited higher level of HGF with respect to SE.

1.3 Conclusions

Despite the fact that these tumours are mostly curable, the increased incidence recorded in the last four decades, correlated with the young age of the patients, make it necessary to have a better understanding of their pathogenesis. It is clear that new therapeutical strategies are needed. In a recent work we already demonstrated that HGF/c-MET system is expressed in TGCTs cell lines, and that HGF administration determines higher biological responses in non-seminoma cell lines. We also showed that these results are in line with *in vivo* studies, where c-MET immunoreactivity is observed, especially in all the most differentiated cancer specimens. To shed light on the onset and progression of TGCTs, herein we demonstrate that c-MET is responsible for the activation of c-Src and PI3K/AKT pathways in non-seminoma cells. Moreover, we show that the HGF expression has a different distribution in SE and in EC, thus suggesting that, very likely, the presence of HGF in testis microenvironment plays a role in the pathogenesis of TGCTs, and especially of EC. Taken together, these results contribute to pave the way for more accurate therapies.

2. Introduction

2.1 Germ Cell Tumours (GCTs)

2.1.1 Classification

Though human testis appears as a relatively small organ, it can give rise to numerous neoplasms, which originate from the various cell lineages that compose the whole organ. Notably, the most frequent neoplasm that occurs in the testis originates from Germ Cells (~95%).

Human Germ Cell Tumours (GCTs) are a heterogeneous group of pathologies that origin in the male and female gonad, and that have been classified for the first time in 1946 by Friedman and Moore (1).

The classification of GCT is based on the developmental potential of these neoplasms. The last classification, published in 2017, replaces the old classification by the same authors in 2005. Nowadays, according to the latest classification, these tumours are divided in seven types and for this reason it differs from the classification in five groups in 2005 (2).

As far as the male gonad is concerned, five of these lesions are considered the most relevant, and, among these, type II Testicular Germ Cell Tumours represent the most common cancers in young men between 15 and 39 years old.

GCT Type	Age Group	Sex	Site	Phenotype	Developmental State
0	Neonates	F/M	Midline	Included and parasitic twins	Omnipotent (2C state)
I	<6 years	F/M	Gonads, midline	TE, YST	Pluripotent (primed state)
II	Postpubertal	>>M	Gonads, midline	SE/Dysg, NST	Totipotent (naïve state)
III	>55 years	M	Testis	ST	Spermatogonium to premeiotic spermatocyte
IV	Postpubertal	F	Ovary	Dermoid cyst	Maternally imprinted 2C state
V	Postpubertal	F	Placenta, uterus	Hydatidiform mole	Paternally imprinted 2C state
VI	>60 years	F/M	Ovary, atypical sites	Resembling type I or NST components of type II	Primed state or NST lineages of naïve state

Table 1: Current Testicular Germ Cell Tumours classification (from João Lobo et al., 2019).

2.1.2 Testicular Germ Cell Tumours (Type II)

Type II GCTs can develop in testis, ovary, brain and mediastinum. Over 90% of type II GCTs occurs in the testis (3). These

neoplasms arise by a common precursor, called “Germ Cell Neoplasia In Situ” (GCNIS). From GCNIS derive both seminoma lesions (SE), and non-seminoma tumours (NST). Approximately, 50% of TGCTs are pure seminoma, whereas 44% are non-seminoma tumours (4). The median age at diagnosis is 33 years-old, specifically 25 for NSTs versus 35 for SEs (5). All type II TGCTs may metastasize to lungs, liver, retroperineal lymph nodes, brain and bone. These tumours show high potential of differentiation (these cancer cells appear often multipotent or totipotent) and the origin of their pathogenesis is probably due to an alteration of the spermatogonial niche. In detail, the differentiation of the germ cells is determined by down-regulation of pluripotency genes and up-regulation of germ cell specific genes. Disturbed Sertoli cells/niche might interfere with downregulation of OCT4, normally co-expressed with TPSY, which respectively protect germ cells from apoptosis and stimulate their proliferation (6).

2.1.3 Origin of Type II TGCTs

The origins of type II TGCTs is still a matter of debate, however the most accredited theory indicates that they derive from the arrest of the differentiation of some gonocytes, during prenatal development. These cells give rise to a pre-cancer lesion, called pre-germ cell neoplasia in situ (pre-GCNIS). This cancer lesion remain quiescent until puberty and in this period acquires genomic alteration; then, hormonal changes, during puberty, lead to complete GCNIS features acquisition (7, 8).

GCNIS, as previously mentioned, is the common precursor of all type II TGCTs. Its nomenclature has changed many times. Niels Skakkebaek was the first researcher that identified abnormal spermatogonia in two different biopsies, both of which develop into cancer. In 1972 Skakkebaek called this lesion carcinoma in situ (CIS). Only starting from 2015 the lesion was identified as GCNIS, when Prof. Leendert Looijenga proposed this term during a meeting in Zurich (9, 10). GCNIS can lead to seminoma tumours characterize by the expression of germ cell specific genes (“default

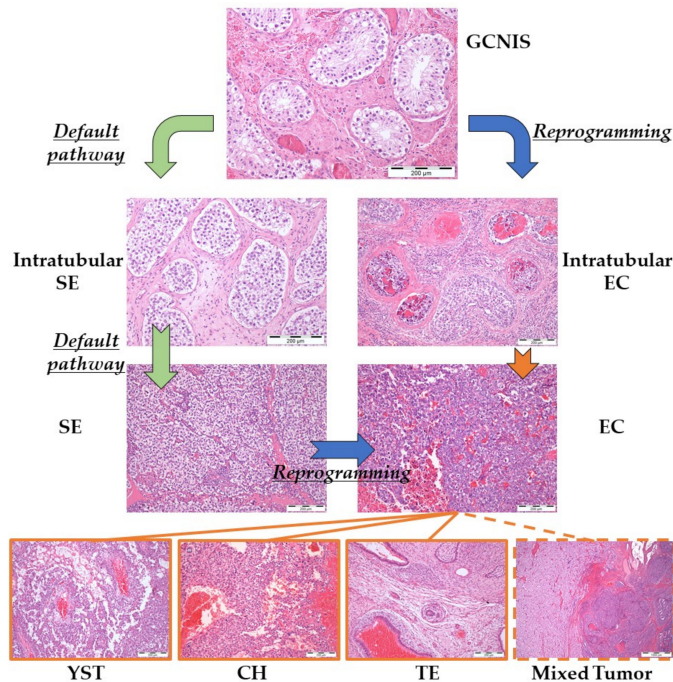


Figure 1: Pathogenesis of type II TGCTs. GCNIS is the common precursor of all type II TGCTs. A genomic reprogramming can occur in GCNIS or, sometimes, in SE. This reprogramming gives rise to EC, a precursor of all types of non-seminoma tumours (from João Lobo et al., 2019).

pathways”) as well as the maintenance of the expression of pluripotency genes. The genetic and epigenetic reprogramming of the GCNIS, or in some cases of the SE, determined the development of the Embryonal Carcinoma (EC) that is featured by the up-regulation of pluripotency genes and consequent down-regulation of the germ cells specific genes. EC is in turn the precursor of all types of non-seminoma tumour, as well as teratomas (TE), choriocarcinomas (CHC), yolk sac tumours (YST) and mixed tumours. Moreover, EC cells can give rise to all lineages of embryogenesis; YST and CHC represent extraembryonic tissues, while teratomas represent somatic tissues

with expression features of all the three germ layers of the developing embryo (2).

The clinical interest about this type of tumours is enhanced in the last decades, due to an increase of their incidence especially in the Western countries, such as Europe, North America, South America, and Australia. In particular, it is worth mentioning that the highest incidence was recorded in Denmark, Norway and Switzerland (11-13). The global incidence is 1.5 affected individuals per 100.000 with difference of 20-times between area with the lowest and higher incidence (14). This non-randomic distribution of these pathologies has suggested that environmental factors, more available in high developed countries, can lead the development of these pathologies. However, the high variety of incidence among different ethnic groups in the same society demonstrate also the genetic relevance in the pathogenesis of these tumors. TGCTs is in fact a notable example of the close relationship between genetic and environmental factor which act in synergy with each other promoting the malignant transformation. The concept that fuses both factors has led to creating a new word called 'genvironment'.

2.1.4 Risk Factor

2.1.4.1 Environmental Risk

Previously mentioned block of the gonocytes is due to an altered microenvironment, which lead to a multivariegate syndromes, as well as the Testicular Dysgenesis Syndrome (TDS), which increase approximately five times the risk to develop TGCTs (15). TDS is considered as a relatively mild disturbance of sex differentiation, due to hypovirilizing factors in utero (16-18). Features of TDS, which confer higher risk to develop TGCTs, include cryptorchidism, previous inguinal hernia, hypospadias, previous testicular cancer (TGCTs are bilateral in 3-4% of the cases), impaired spermatogenesis and familial history of testicular type II GCT.

Beside, other important risk factors in the onset of TGCTs are considered the low birthweight, short gestational age, twin, tall stature, first born child and disturbed hormonal conditions in utero (2).

Literature data demonstrated contrasting hypotheses but it seems that in the pathogenesis of type II TGCTs contribute also external environmental risk factor which act post-natally, such as diet (in particular the use of high in fat and dairy products), exposure to hormone disruptive organochlorine insecticides which influences the masculinization process, or a jobs like fire-fighting and aircraft- maintenance. Cannabis smoking is also considered a risk factor for the onset of TGCTs, and, in particular, it seems to be involved predominantly in the non-seminoma development. The last overview highlights that cannabis smoking can promote the reprogramming of seminoma tumours (19-25).

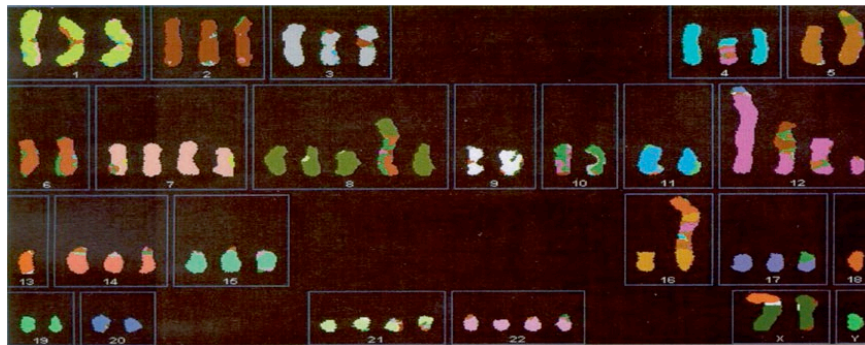


Figure 3: Spectral karyotype of type II GCT. Normally each chromosome have a specific color, but appears clear that chromosome 12 contains other chromosome fragments (from Oosterhuis H.W. and Looijenga L.H.J., Pathology and Biology of Human Germ Cell Tumors, Nogales, R.E. Jimenez (eds.), Springer-Verlag GmbH, Germany 2017).

2.1.4.2 Genetic Risk

A hallmark of type II TGCTs is their poliploidy. One of the peculiarity of their chromosome remodelling is the presence of duplication of the short arm of chromosome 12, frequently present

as isochromosome 12p (7, 26-28). On chromosome 12 are localized *NANOG* and *STELLAR*, genes that are involved in the maintenance of pluripotency, and *cyclin D2* gene that regulates positively cell proliferation (29). Therefore, the gain of function of chromosome 12 promotes the block of differentiation of gonocytes as well as the increase of their proliferation. In addition, it has been reported that TGCTs are characterized also by other genomic aberrations that are the duplication of chromosomes 7, 8, 14, 15, 17 and X (30-32). Among them, the mentioned gain of 17q is frequent in non-seminoma tumours (33, 34).

In spite of all these chromosomal anomalies, there are few gene mutations identified as a risk factor for the onset and progression of TGCTs. However, it should be highlighted that mutations of *KIT* gene and the de-regulation of KIT/KITL pathway, important in the PGC/gonocyte survival and migration, represents one of the risk factor for the onset of TGCTs. This de-regulation is peculiar in particular in the seminoma tumors (35-37). Somatic mutations of *KRAS* and *NRAS* genes have been found both in seminoma and non-seminoma lesion, as observed in other solid tumours. Moreover, very recently, a mutation of PDE11A (phosphodiesterase 11A) was discovered in a familial form of this pathologies. Notably, in sporadic cases, the de-regulation of sex determination/germ cell specification, as *DMRT1* and *TPSY* genes are involved in TGCTs pathogenesis (38, 39). Disorders of sex development (DSD, in its more aggressive form: 46,XY, characterize by atypical development of the gonads, sexual organs and/or secondary sex characteristics and considered as the most severe form of TDS), is also implicated in the onset of TGCTs. Essentially a defect in any gene involved in gonadal development and sex differentiation may cause DSD. These defects are considered to affect gonadal development and increasing the risk for GCNIS and TGCT. An example is the mutation in *AR* gene, related to DSD, that are associated with high risk of germ cell neoplasia (15, 18). Furthermore, it is known that a deletion in azoospermia factor c region of Y (AZF) represent a risk factor in

TGCTs oncogenesis (40, 41). Finally, Insulin-like growth factor receptor-1 (IGF1R) has an important role in the proliferation and survival of the PGCs and gonocytes. In a recent study phosphorylation of IGF1R was found in non-seminoma cell lines and was observed that it can promote acquired cisplatin resistance in non-seminoma cells (42, 43).

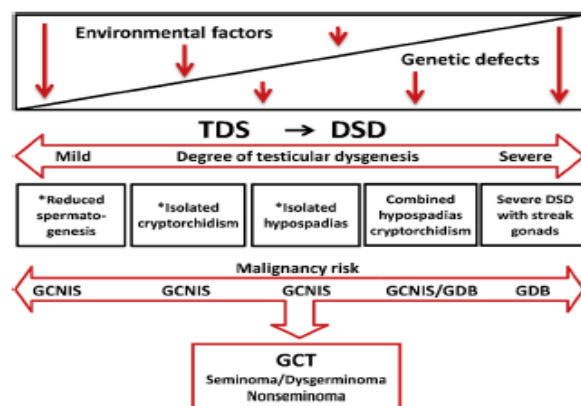


Figure 3: Schematic representation of the pathogenesis of germ cell tumours (GCT). The implication of testicular dysgenesis syndrome (TDS), predominantly caused by environmental factors, and DSD predominantly genetically determined, in GCT pathogenesis are shown. (from Jorgansen Anne et al.; 2015).

2.1.4.3 Epigenetics

With greater understanding on onset and progression of TGCTs, epigenetic acquired more and more importance. Study of type II TGCTs demonstrated that they are characterized by demethylation and erasure of parental imprinting. In fact, during the embryonic period, the Primordial Germ Cells (PGCs) are imprinted with female features. When testis develop, PGCs surrounded by Sertoli cells become pre-spermatogoni and went to a de-methylation process. After that a "new primary metilation" is generated. This mechanism is sex-dependent, hence the genome of male and female gametes has different metylation patterns. In the de-methylation period the cell is more sensitive to mutational events.

Several studies demonstrated that serum of patients affected by type II TGCTs showed epigenetic alteration in correlation with healthy samples, and methylation of *BRCAl* or *RAD51C* genes are only few examples of the implication of epigenetics in the TGCTs pathogenesis (2, 44-46).

2.1.4.4 *Genvironmental hypotesis*

The interplay between environmental and genetic risk is called “Genvironmental hypotesis”. These pathologies represent in an exemplary way the interchange between the environment and genetic and epigenetic factors in the development and progression of the disease.

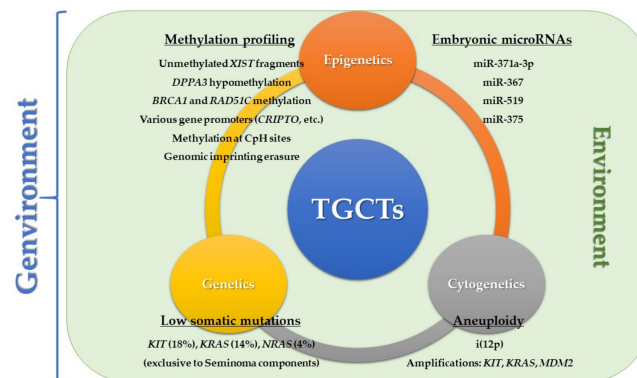


Figure 4: Genvironmental Hypotesis. Representation of the genvironmental model focused on genetic, cytogenetic, and epigenetic factors, which are continuously modified and conditioned by environment (from João Lobo et al., 2019).

2.1.5 *Chemo- and radio- resistance acquisition*

Nowadays, testicular germ cells tumors are among the most curable solid tumors existent, with an average of 95% patients survival in the 10 years following the therapies (47, 48). The gold standard of the therapy in use for these tumors is based on a combination of radio- and chemo- therapy, with surgical removal. This protocol normally offers a good prognosis. Although, a little percentage of patients affected by TGCTs (approximately 5-10%)

developed resistance or long-term toxicity of the treatment previously described. Although these data seem positive, TGCTs represent the major cause of death in young men between 15-39 years old. . Because of the young age of the TGCTs onset, they have become cause of concern for the world cancer community.

The most widely used chemotherapy protocols includes: BEP (bleomycin, etoposide, and cisplatin), EP (etoposide, cisplatin) and VIP (cisplatin, etoposide, ifosfamide) and the majority of the patients are treated with high doses of these drugs (49). As a consequence, patients can develop long terms toxicity due to at high cisplatin doses find in the plasma and urine also after years (50). The long-term toxicity can give origin to several diseases, as peripheral neuropathy, ototoxicity, secondary malignancies, cardiovascular toxicity, renal or pulmonary toxicity and infertility. On the other hand, other patients developed drug resistance with unclear mechanism. This acquired resistance kills about 5% of the patients. Even if the mechanism of resistance has been only partially elucidated, one of the hypotheses that are commonly considered is the decreasing of the cysplatin-dependant repair mechanism after DNA damage. TGCT patients show decreasing of these repair systems. Other supposed mechanisms of drug resistance are hypothesized, firstly the inactivation of p53 or de-regulation of PI3K/AKT pathway. In fact, normally p53 is not mutated in TGCTs patients even if they show high expression of MDM2, the principal physiologic antagonist of p53. Moreover, in EC it was observed high expression of OCT4 related with high expression of NOXA (Bcl-2 family member), suggest the involvement of OCT4 in the escape mechanism of apoptosis resistance-related drug (51).

Taken together, from these observations it appears clear that a better understanding of the onset and progression of these types of tumour are needed to make up new personalized therapies in order to improve quality of treatments and long-term status of the patients.

2.1.6 Cell lines and models

Type II TGCTs are probably unique in humans. In fact, no convincing examples of spontaneous or induced type II TGCTs have been reported in animals. The long time required for all the oncogenic steps may explain why there are no evidences of these pathologies in other animal models.

Regarding seminoma tumours, there is only one experimental model, called TCam-2 cell line, derived from a human primary TGCT with a seminoma component. This cell line is characterized by the expression of specific seminoma tumours markers, as well as NANOG and c-KIT, in combination with SOX17 (52, 53).

Instead, there are some cell lines representative of non-seminoma tumours. The first established and well-characterized non-seminoma cell line is NT2D1. This cell line, used in my work, is a sub-clone (D1) derived from a human pluripotent embryonal carcinoma parent line NTERA-2. In turn, this cell line was established from a nude mouse xenograft tumour of TERA-2 cells, which were isolated from a lung metastasis of a 22 years old patient with primary embryonal carcinoma of the testis. NT2D1 cells express pluripotency genes, among which *SOX2*, *OCT4* and *NANOG* (53). Noteworthy, they are negative for SOX17, specific for seminoma tumours. NT2D1 is widely used to study EC differentiation, in fact when this cell line is cultured at low density can differentiate, while at high density their pluripotency is maintained.

2.2 HGF/c-MET system

2.2.1 Hepatocyte Growth Factor (HGF)

The Hepatocyte Growth Factor (HGF), also known as Scatter Factor (SF), was described for the first time in 1989 (54).

It belongs to serin protease super-family, and it is normally secreted by cells of mesenchymal origins. Moreover, it acts as a pleiotropic factor and cytokine promoting cell motility, survival, proliferation, differentiation and morphogenesis. HGF is secreted as a single-chain precursor and its activation is regulated at post-translational level. In fact, the single chain precursor is converted in

an active form, a two-chain functional heterodimer extracellular protease, by an extracellular protease called HGF activator (HGFA) as well as the type II transmembrane enzymes metriptase and hepsin. It is also related to urokinase plasminogen activator (uPA) and tissue plasminogen activator (tPA) that are able to convert pro-HGF in two chain HGF. Active HGF form is composed by an α -chain of 69 kDa that binds a β -chain of 34 kDa through a disulfide bond. The α -chain is formed by an hairpin loop and four kringle domains, while β -chain is characterized by a serine protease homology domain which lacks proteolytic activity (55, 56).

Activation of HGF is finely regulated by the expression and secretion of two potent inhibitors of HGF activator known as HGF activator inhibitor 1 (HAI1 also known as SPINT1) and HGF activator inhibitor 2 (HAI2 or SPINT2).

2.2.2 Mesenchymal Epithelial Transition (c-MET)

c-MET is a member of receptor tyrosine kinases (RTKs) family, first discovered in 1984 (57) and normally expressed on the surface of epithelial cells. This receptor has a significant morphogenic and mitogenic role and it is essential during embryogenesis. It is also important in the adult life during wound healing, tissue repair, and homeostasis. In humans the proto-oncogene is located at 7q21q31 chromosome. The gene encoded for a single chain precursor of 150 kDa and, after translation, a glycosylation and a proteolytic cleavage are involved in the Golgi apparatus in the maturation of the receptor. The mature form of c-MET is a heterodimer of 190 kDa and it is composed by an α -chain of 50 kDa and a transmembrane β -chain of 145 kDa linked by disulfide bonds. The extracellular region is formed by three functional domains, which include: 1) the, Sema domain at the N-terminus site, that includes the whole α -chain and part of β -chain; 2) PSI (plexin, semaphorine and integrin cysteine-rich) domain; 3) and four IPT (immunoglobulin plexin transcription) domains. The intracellular domain contains a catalytic region, a juxtamembrane sequence and a carboxy-terminal

multifunctional docking site. (58). The binding of HGF to the Sema domain of c-MET receptor triggers two different phosphorylations in the c-MET intracytoplasmic tail: the first is the trans-phosphorylation of Tyr1234 and Tyr1235 residues, responsible of the kinase activity, whereas the second is the phosphorylation in the docking site at Tyr1349 and Tyr1356, responsible for the recruitment of several molecular adaptors (59).

In the juxtamembrane domain there are two residues, Ser 975 (that inhibits the c-MET receptor after its phosphorylation) and Tyr1003 (that interact with cbl), both implicated in the downregulation of the receptor: c-MET is ubiquitinated through the action of cbl (E3 ubiquitin ligase casitas B lineage lymphoma). Cbl is able to attract ubiquitin-loaded E2 molecules, which are responsible for the tag of the receptor with ubiquitin. This way, it can be sorted into clathrin-coated areas on the plasma membrane. Subsequently, it undergoes lysosomal degradation. At the same time, cbl may determine membrane recycling (60). Receptor-mediated endocytosis is required for the full activation of c-MET signaling pathway and consequently for the various cellular responses (61-63). Moreover, it is known that c-MET degradation can occur through several mechanisms. One of this is the ubiquitination as previously mentioned. Moreover, it is also been demonstrated another mechanism which involve ADAM metalloprotease, that determines the shedding of the c-MET ectodomain and the proteasome degradation of the cytoplasmic tail (59).

On the other hand, c-MET has several truncated isoforms generated by post-translational processing or alternative splicing. In particular, two isoforms are described, one is the isoform of 130 kDa, and the other is the isoform of 140 kDa, both without the tyrosin kinase domain. While the 130 kDa isoform were released from the cells, the other one is localized on the cell surface (64). Nowadays, the specific biological function of these c-MET truncated isoforms is unknown. One of the mechanism proposed described that these isoforms can prevent the full length c-MET activation blocking HGF. But also other mechanisms are proposed,

for example the loss of function in the Cbl-binding region which determine impaired of the c-MET downregulation (59, 65, 66).

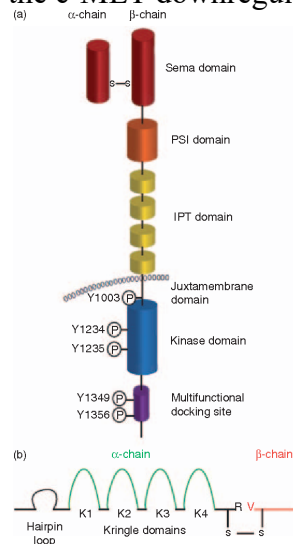


Figure 5: General Structure of c-MET Receptor (a) and its ligand HGF (b) described in detail in the text (Organ and Tsao, 2014)

2.2.3 HGF/c-MET signal transduction

The binding of HGF to its unique receptor, c-MET, starts a complex signal transduction cascade. First of all, this event determines a conformational change of the receptor that in turn determines a dimerization of the receptor. Subsequently, two phosphorylation events occur in the receptor tail, as previously described. The last phosphorylations, which create a SH2 recognition motif unique to c-MET, are responsible for the recruitment of several adaptors responsible of different biological responses. Among these, there are various cytoplasmic effector proteins including phospholipase C (PLC), phosphatidylinositol 3-kinase (PI3K), Signal Transducer and Activator of Transcription (STAT3) and the non-receptor tyrosine-kinase Src which are recruited by active c-MET. Frequently, these proteins are directly phosphorylated in tyrosine by the receptor. Moreover, there are several adaptor proteins, as well as Growth Factor Receptor-bound

2 (GRB2), Src homology-2-containing (SHC) and GRB2 Associated Binding Protein (GAB1), a multi-adaptor protein that creates binding sites for different downstream pathways.

c-MET downstream responses are similar to other RTKs. There are canonical pathways that transmit biochemical information from the cell surface, where c-MET resides, to the nucleus. The receptor through PI3K results in the formation of phosphatidylinositol 3,4,5-triphosphate (PIP3) which binds pleckstrin homology domain (PH domain) of AKT (Ser/Thr kinase) to the plasma membrane (in correspondence with PIP3) and this event determined several cell-dependant responses, such as anti-apoptotic signals, with the inactivation of Bcl-2 and the activation of MDM2 (promoting p53 degradation), or promoting survival responses activating the mammalian target of rapamycin mTOR, as well as the AKT-dependant inactivation of GSK3 β determined the downregulation of the cell cycle regulator, like cyclin D1 or Myc (59). c-MET can also activate MAPK cascade. Through molecular adaptors, previously described, it generates the activation of the sarcoma viral oncogene homology (RAS) that leads to the activation of RAF kinase that in turn can activate Mitogen Activated Protein Kinases (MAPKs) cascades (59) involved in proliferation, cell cycle progression or cell motility. c-Src is also activated by c-MET and this molecule normally determined the phosphorylation of Focal Adesion Kinases (FAK) implicated in migration and invasion processes (58). The role of STAT-3 is widely described, and it is well known that c-MET active determined directly the phosphorylation, dimerization and traslocation in the nucleus resulting in invasiveness responses (67) or in tubulogenesis (68).

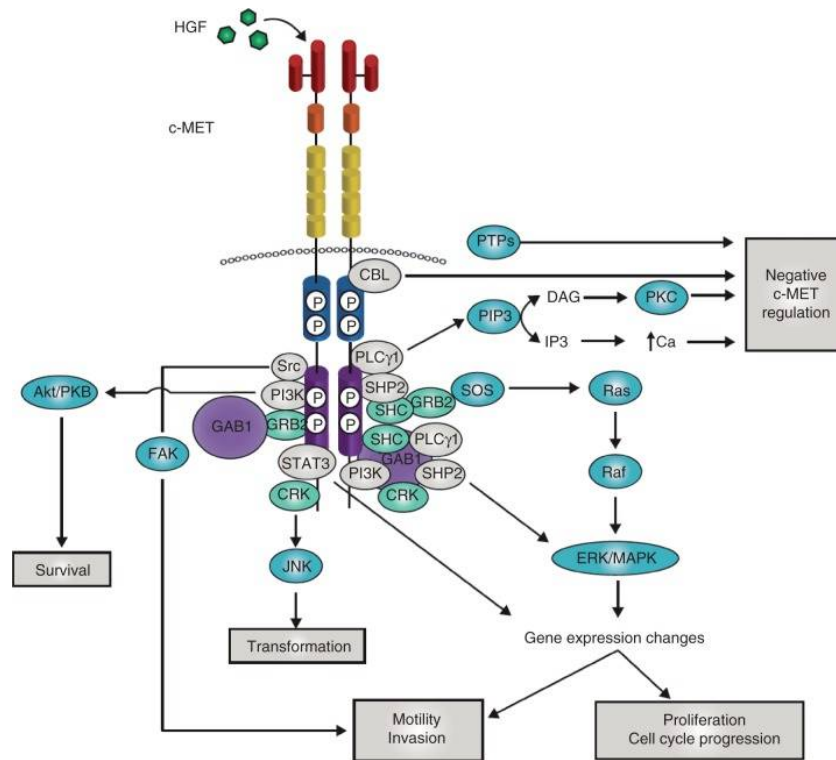


Figure 6: HGF/c-MET pathway. HGF binding determine c-MET dimerization and activation. Several molecular adaptors are recruited, which directly or indirectly interact with c-MET. As a consequence, downstream pathways are, in turn, activated and responsible of various biological responses (Organ and Tsao, 2014).

Nevertheless, it should be mentioned that, c-MET can be activated also in an HGF-independent manner. Literature data demonstrated different biological crosstalks among c-MET and other RTKs, other receptors physically associated with it at the cell surface. These crosstalks are object of several studies for the emerging role in the development of drug resistance in target therapies. It has been found in fact, that some RTK (as well as VEGFR and EGFR) activated by their ligands can bind c-MET, determining its phosphorylation. It is possible even that c-MET activated by HGF

can dimerize with other RTKs activating their signalling pathways. In both cases, signal transduction amplification occurs (58). It is also worth mentioning that, the hyaluronan receptor (CD44) can bind c-MET lead to the activation of RAS/ERK signaling through SOS recruitment and binds c-MET to the cytoskeleton (59, 69). The relationship between c-MET and the Epidermal Growth Factor receptor (EGFR) is widely provided, as well as its link with the Transforming Growth Factor (TGF- α) (70, 71). Even the binding with laminin receptor- $\alpha 6\beta 4$ integrin, or with semaphorin receptors of plexin B family or the linking with Vascular Endothelial Growth Factor Receptor (VEGFR-2) are proved (72). These events determined the synergistic activation of the downstream RTKs related pathways.

2.2.4 HGF/c-MET in testis

c-MET has an essential role in embryonic development, as demonstrated by the lethal phenotype observed in *c-MET* knock-out mice due to several placental defects. This observation led to deeper investigate HGF/c-MET system during prenatal phases, Notably, it has been found expressed and active during all phases of pre-natal and post-natal development of several organs whose morphogenesis appears regulated by a tight epithelium-mesenchyme cross-talk. Gonads can be numbered among these organs. Studying the mouse embryo, in fact, HGF/c-MET system has been detected in the urogenital ridge since 11.5 dies post coitum (dpc), and it probably collaborates with other growth factor, such as FGF9 and PDGF, in driving the sex-specific cells migration of mesonephric cells toward the developing testis (73-75). HGF/c-MET system is also involved in Fetal Leydig cell development starting from 15.5 dpc, regulating their endocrine function, differentiation and survival (76, 77).

In rat post-natal testis c-MET receptor has been found expressed in all the main cell lineages, including germ cells, even if at different levels and in different phases of testicular post-natal development (78). In this animal model HGF has been found to exert several

functions: it is involved in Sertoli polarization and differentiation; it promotes survival and endocrine function of Adult Leydig cells; it is involved in the regulation of cytoskeletal organization of myoid cells (79-82); it regulates sperm motility (78).

Few data are available on HGF/c-MET system expression and role in human testis. Among them, in 1996 the expression of the receptor was described in human testicular tissue, in particular in the germ cells (83). The same group after two years identified also the expression of its ligand HGF, and they observed altered levels of HGF in the seminal fluid of patients with andrological disease (84).

2.2.5 HGF/c-MET de-regulation in human cancer

HGF/c-MET system is very important for tissue development and homeostasis, and then it is not surprising that its de-regulation has been observed in several human cancers, being associated with aggressive pathologic features, poor prognosis and treatment resistance (85). Aberrant c-MET signaling in human malignancies can occur by a variety of mechanisms. Among these, a copy number increase of c-MET was found in several of neoplasias, associated with a gene amplification with higher *c-MET* gene level. An example of this mechanism is observable in the non-small cell lung cancer (NSCLC) and high level of c-MET protein has been associated with a decrease of patients survival. Mutation of the *c-MET* gene represents a not so frequent event in cancer, although it is well demonstrated that in some cases it represents a pivotal role in the carcinogenesis. There are several mechanisms of activating mutations described, in particular, for instance missense mutations in the catalytic domain of c-MET determines the constitutively activation of the receptor. This kind of mutation has been observed in hereditary and sporadic forms of papillary renal cell carcinoma (86, 87), in childhood hepatocellular carcinoma (88), and in rarely other cancer types. Moreover, somatic mutations were also observed in the juxtamembrane domain of c-MET, necessary for the recruitment of the E3-ubiquitin protein ligase Cbl, resulting in

the accumulation of the receptor. In 2002 it was described that somatic c-MET mutations that constitutively activate its signalling are frequent at metastatic sites. This observation strongly indicates the tight relationship between c-MET activation and cancer progression (89). Another mechanism, which is involved in constitutive activation of c-MET, is the increased secretion of HGF by tumour cells or intrinsically by stroma. This event is observable in glioma, osteosarcoma, pancreatic breast and gastric cancers (90, 91).

Functional crosstalk between c-MET and other receptors results in an emerging important mechanism implicated in cancer progression and drug resistance (66). The dimerization with c-MET and IGF1R, EGFR, ERBB2 or VEGFR and others has also been studied in several human cancers.

2.2.5.1 Cancer treatments and HGF/c-MET

As previously stated, de-regulation of HGF/c-MET system is frequently observed in many tumours and the activation of this signaling determined more aggressive clinical behaviour with higher invasion, metastasis and acquired drug resistance. It has become evident that tumour microenvironment acquired a very important role in the onset and progression. In fact, it is well known that important changes occur during carcinogenesis and tumours are able to create an environment suitable for tumour maintenance. Cytokines, growth factors and chemokines secreted by stromal cells are fundamental in these processes (71).

RTKs have become very attractive drug targets in the development of novel treatment strategies. Moreover, as previously described, HGF/c-MET system is an intricate and highly regulated signalling in the cells. Within this view, c-MET is a promising specific target and it is used in different cancer therapies (92). Nowadays, a number of strategies targeting the HGF/c-MET axis are in development. These approaches use respectively HGF or c-MET as a target.

Among the first category, we distinguish HGF activation inhibitors (preventing the activation from pro-HGF to its active form) and HGF inhibitors (preventing the binding between HGF to c-MET receptor). The activation of HGF depends on the balance between the activators (HGFAs) and inhibitors (HAIs) and this may represent a new interesting target, but the development of HAIs is in the early stages. Regarding HGF inhibitors, several antibodies against this growth factor are tested and among these Ficlaturumab and Rilotumumab, two monoclonal antibodies, are used in different clinical trials (85).

As for the second category, c-MET antagonists (which compete with HGF for receptor binding) or c-MET kinase inhibitor were identified (85, 93). c-MET antagonist compete with HGF for c-MET binding causing the degradation of the receptor and its inactivation. Onartuzumab is an example of these and it is in phase III in the treatment of NSCLC and phase II of breast cancer. Regarding c-MET kinase inhibitor, we can distinguish c-MET selective small molecules, such as Tivantinib in several clinical trials in phase I, II, and III or Savolitinib that displayed in vitro activity against c-MET. Among c-MET non selective drugs we found Foretinib, Cabozantinib and Crizotinib, all of these demonstrate an additional activity against other receptors. These drugs are in pre-clinical and clinical studies and patients are consistently recruited for different phases of anti-tumour therapies (<http://www.clinicaltrials.gov;2013>).

Nowadays, it is well known that c-MET is implicated in the resistance to target therapies, including approved EGFR inhibitors (94, 95). Treatment with monoclonal antibody against EGFR are used in several solid tumors and generally acquired resistance appears in 3-12 month after treatment. Some of these mechanisms of resistance are dependant on the amplification of c-MET. Cetuximab resistance in colon cancer cells was observed and this cellular response is related to an up-regulation of p-c-MET. Na Song et al. described that in in-sensitive Caco-2 cells active c-MET was found and this activation is involved in the escape from the

inhibitory effect of cetuximab (95, 96). This effect was reverted using a c-MET inhibitor which is able to restore cetuximab responses. In the same work it is also demonstrated that p-c-Src is related to p-c-MET in Caco-2 cells and c-Src activation cooperate in the cetuximab resistance activating in turn PI3K/AKT or ERK pathways as effectors (96). Biologic agents targeting the VEGF pathway have also produced significant clinical benefits in some cancers but drug responses are usually short-lived. Inevitably, drug resistance emerges. In fact, HGF/c-MET axis appears important also in acquired VEGFR inhibitor resistance and vascular remodeling in non-small cell lung cancer (NSCLC) (97). In summary, tumour microenvironment sustained cancer progression. HGF/c-MET axis results up-regulated after TKIs therapies and this event results implicated in drug resistance. Recently, it was observed that cancer associated fibroblasts (CAFs) produce HGF which sustaining adaptive resistance to targeted therapies (98). These evidences shed new light on the novel combined target therapies development and combinatorial TKIs and HGF/c-MET targeting may represent a reasonable approach to improve patient outcomes.

2.3 c-MET in TGCTs

The possible role of c-MET in TGCT pathogenesis is still a matter of debate, since literature data on this subject is very poor. To this regard, in 1996 Mostert and collaborators described a gain of chromosome 7 in primary tumours of patients affected by TGCTs (99). Moreover, another work published in 2004 mutation for c-MET have not been reported in TGCTs (100). Svetloska et al. analyzed several circulating cytokines, among which HGF, in the serum plasma of patients affected by TGCTs and an inverse correlation between higher HGF level and good prognosis was demonstrated (101).

2.3.2 My previous work

Recently, my group observed the differential expression of c-MET in cell lines derives from patients affected by seminoma and non-seminoma tumours (TCam-2, NCCIT and NT2D1 cells). In this work we demonstrated that non-seminoma cell lines (NT2D1) show the higher cellular responses to HGF administration, with respect to the other cell lines, in terms of proliferation, invasion and migration. In line with these results we also observed, in human biopsies, that non-seminoma cancer lesion exhibit c-MET at higher levels with respect to GCNIS and seminoma lesions (102).

Starting from these evidences, my group and I decided to analyze c-MET-activated pathways by HGF administration in NT2D1 cells. In particular, we focused on c-Src and PI3K dependent pathways triggered by c-MET activation. The results obtained on the analysis of c-Src activation, that I will report in this thesis, has been recently published. A graphical representation is shown in Figure 7 (103). The data focused on PI3K signalling belong to a manuscript in preparation.

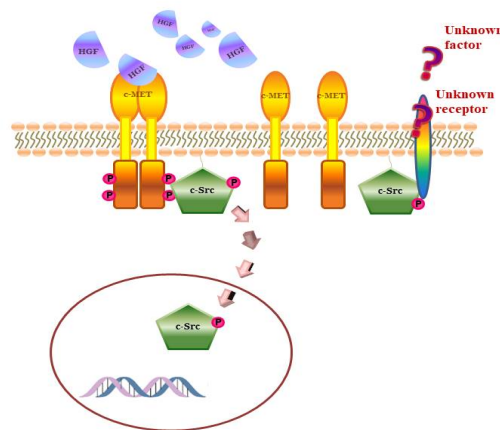


Figure 7: Graphical abstract. HGF administration in NT2D1 cells determines activation of c-MET. It can activate c-Src protein, which changes its localization and translocates in the nucleus. This phenomenon is responsible for NT2D1

Erica Leonetti

biological responses, such as proliferation, migration and invasion. In this system c-Src can also be activated by an unknown factor, without HGF/c-MET involvement. This results in higher collective migration and invasion (from Leonetti E. et al., 2019).

3. Aims

HGF/c-MET system has a very intricate signalling whose importance is well known during embryogenesis. c-MET deregulation is widely described in several human cancers, and for this purpose, it is used as a target in several personalized therapies (www.vai.org/met). Though, few data are present in literature about this system in TGCTs. *c-MET* is encoded on chromosome 7, region 7q31. A duplication of this chromosome was described in TGCT patients. Noteworthy, high levels of HGF in serum plasma of patients affected by TGCT were found.

TGCTs are a group of pathologies that arise from altered testicular niche during embryogenesis. This alteration is responsible for a block of gonocyte differentiation, which can give rise to all type II TGCTs. TGCTs are mostly curable, but there is still a little percentage of patients who develop drug resistance, radio-resistance, or long-term toxicity due to the used chemo- and radio-therapy. For these reasons, as well as for the young age of the patients and the increasing incidence in recent years, it is a paramount to have a better understanding on the onset and progression of TGCTs.

In a previous work we demonstrated that c-MET is expressed by several cell lines derived from type II TGCTs and that HGF administration determines strong biological responses, especially in non-seminoma cell lines. In line with these results, we also observed that c-MET was present in human biopsies derived from patients affected by all type II TGCTs (102). In order to better characterize onset and progression of TGCTs, we decided to investigate:

- 1) The specific role of the c-MET receptor in chemotaxis and collective migration (continuing the previous work).
- 2) The signalling pathways triggered by HGF and mediated by c-MET activation, by identifying the main adaptor proteins related to it in NT2D1 cells and their role.
- 3) The synergic relationship among different activated adaptors in NT2D1 cells.

Erica Leonetti

- 4) The differential HGF expression in biopsies derived from patients affected by type II TGCTs with specific concern on SE and EC.

4. Results

4.1 c-MET modulates the migration of NT2D1 cells induced by HGF

4.1.1 NT2D1 chemo-attraction is specifically driven by c-MET

We previously demonstrated that HGF is a chemoattractant for NT2D1 (102). To deeper investigate the specificity of this cellular response, we performed HGF-activated chemotaxis assays using the c-MET inhibitor PF-04217903 (Figure 8) as described in "Materials and Methods" section. As expected, a significant increase of migrated cells was observed using HGF (40 ng/ml) with respect to the control condition ($2 \pm 0,3$ vs 1 ± 0.13 respectively; $p < 0,001$).

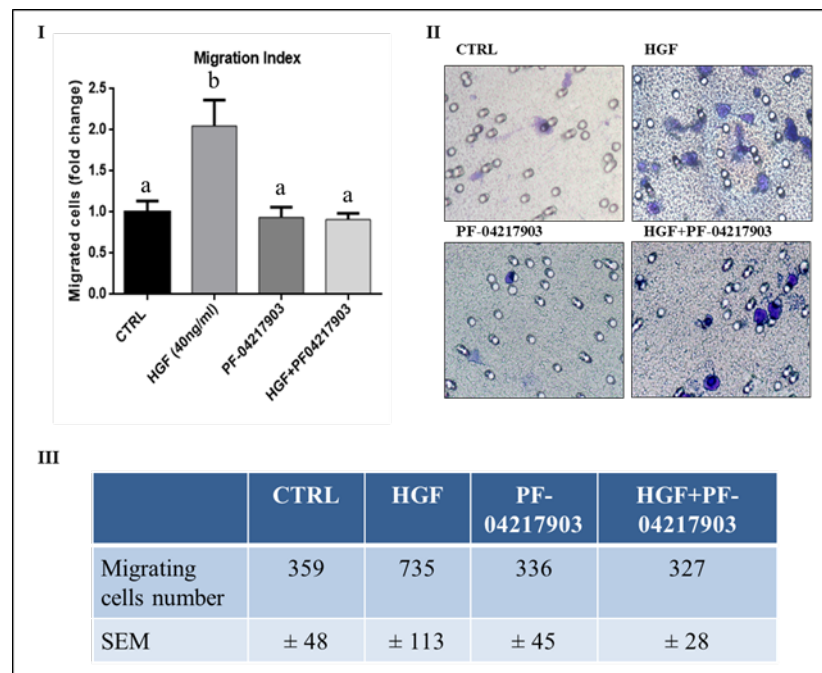


Figure 8: Effect of PF-04217903 on HGF-dependent NT2D1 chemotaxis. Three independent experiments were performed. All experiments were performed at least in quadruplicate. **I)** Graphical representation of the amount of chemo-attracted NT2D1 cells. A significant increase of migrated cells using

HGF was observed (b vs a; $p < 0.001$). The use of PF-04217903 in combination with HGF, abrogates the effect induced by HGF. Control condition was arbitrarily considered as 1, and the values were calculated as “fold change” compared with control (\pm S.E.M.). **II)** Representative images of NT2D1 migration experiments obtained with Diff quick staining. The images were recorded at 40X magnification. **III)** Table illustrating the number of migrating cells/filter in all the experimental conditions reported in the respective “fold change”.

Notably, PF-04217903 alone does not modify the migratory capability of NT2D1 cells compared to the control (0.94 ± 0.12 vs $1 \pm 0,13$ respectively; $p = \text{n.s.}$), whereas the co-administration of HGF+PF-04217903 causes the reversion of the HGF-induced chemotactic effect (0.91 ± 0.08 vs $2 \pm 0,31$ respectively; $p < 0,001$) (Figure 8, panel I). Taken together, these results indicate that HGF-induced chemotaxis is specifically activated by c-MET.

4.1.2a c-MET modulates the collective migration of NT2D1 cells induced by HGF

We analysed in detail the effects of HGF on the collective motility of NT2D1 through wound healing assays performed as described in "Materials and Methods" section. We calculated by Image J v 1.47h software the percentage of the open surface residual area of each experimental condition in correlation with baseline points T0, considered as 100% open area. We did not observe any reduction of open residual area in the wells treated with HGF with respect to control wells after 24 hours from insert removal. After 48h of culture the open area of HGF treated cells resulted significantly reduced compared to the open area of the control condition. This result demonstrates that HGF induces in NT2D1 cells an increase of migration capabilities.

To evaluate the specificity of HGF/c-MET response, we performed the experiments in presence of the c-MET inhibitor PF-04217903. The inhibitor alone results similar to the control condition after 24 and 48h the insert removal. After 24h of culture the open residual area of PF-04217903+HGF treated wells was not significantly different from the open residual area of all conditions, while after

48h of culture the open residual area of PF-04217903+HGF treated wells was similar to the control conditions and significantly higher than the open area of HGF treated wells ($41,1\% \pm 9$ vs $10,4\% \pm 6$ respectively; $p < 0,01$) (Figure 9). These data indicate that c-MET inhibition with the ATP-competitor PF-04217903 significantly reduces (about 30%) the migratory effect induced by HGF. Taken together our results reveal that HGF treatment is able to enhance the collective migration of NT2D1 cells and confirm that this response is specifically dependent on c-MET.

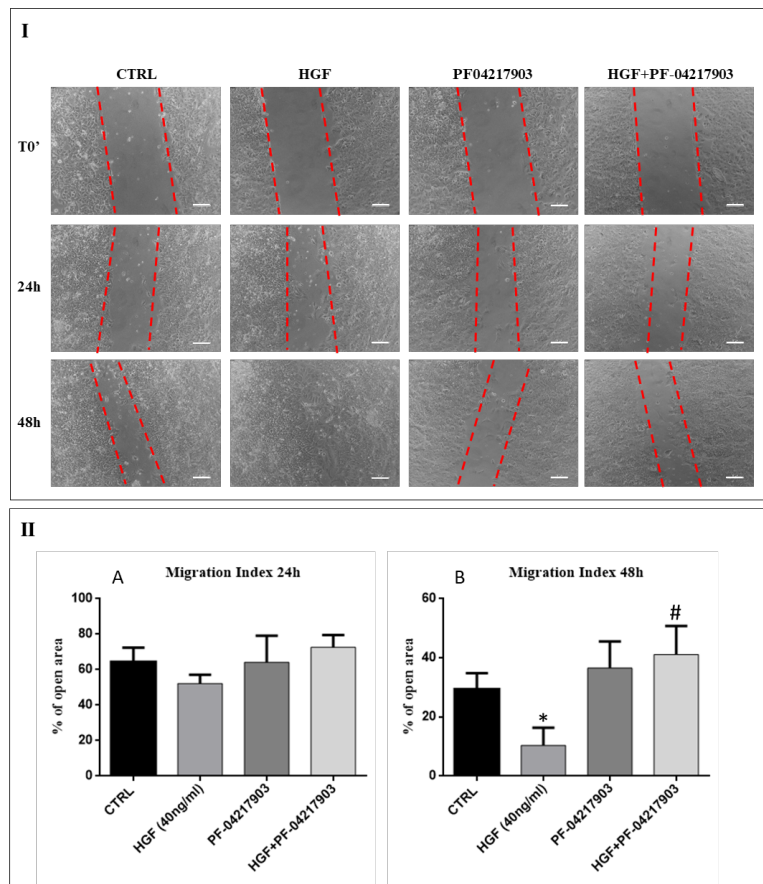


Figure 9: Role of HGF/c-MET system on NT2D1 cells collective motility. Wound healing assay after cells treatment with fresh 2% FBS DMEM (CTRL)

or containing HGF alone, PF-04217903 or HGF+ PF-04217903. Three independent experiments were performed at least in triplicate. **I)** Representative phase contrast images of wound healing assay recovered immediately after insert removal for baseline wound measurement (T0) and 24h and 48h after wounding. Images were photographed at 10X magnification (scale bar: 100 μm). **II)** Quantitative analysis of wound closure after 24h (A) and 48h (B). Data are expressed as the mean percentage of residual open area compared to the respective cell-free surface recovered at T0. After 24h the difference of open area was not statistically significant in all the considered experimental conditions. After 48h the decrease of open area in HGF treated cells was statistically significant with respect to the control (* $p < 0.05$). PF-04217903 alone was similar to the control while PF-04217903+ HGF abrogated the HGF induced effect (# $p < 0.01$).

4.1.2b Proliferation does not affect collective migration induced by HGF

Since HGF is able to promote NT2D1 cell proliferation, as above reported, we wanted to check whether the observed HGF-mediated increase in the rate of wound closure were due to a trigger to cell proliferation rather than to an actual migratory effect. To this end we performed immunofluorescence experiments, using the phosphohistone H3 (pHH3) as mitotic marker, on wound-healing samples at the end of their culture time. To quantify the immunofluorescence results, samples were recovered using the Leica Confocal microscopy (Figure 10, Panel A and B) and analysed by Leica Confocal Software (Figure 10, Panel C). The Sum of Fluorescence Intensity (SUM (I)) of pHH3 signal (FITC/green signal) and nuclei staining (TO-PRO3/blue signal) was calculated in three different areas of each sample. The analysed areas were:

- 1) the whole photographic-field of each wound area (562,500 μm^2 for each image), data reported in Table 1;
- 2) the presumptive wound area (263,486 μm^2 ; inside the dotted lines of the representative images of panel A) data reported in Table 2;
- 3) the confluent areas recovered far from the wound (562,500 μm^2) data reported in Table 3;

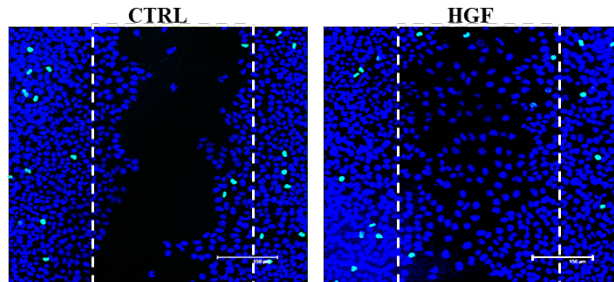
We also counted the pHH3⁺ cells in each area and even these results are reported in data reported in Tables in figure 10, panel C. The values reported in Table 1 clearly show that the SUM(I) analysis as well as the count of PHH3⁺ cells did not reveal any increase of pHH3⁺ cell in the whole photographic-field of wound area (562,500 μm^2) both in control condition and in HGF treated samples.

In Table 2, the values reported show that there is not a significant difference in the amount of pHH3⁺ cells between control and HGF treated cells in the areas of the wound. Notably, an increase of blue fluorescence (that represents nuclear staining) is observable between control condition and HGF treated cells. Altogether these observations indicate that HGF stimulates the NT2D1 cells collective migration and that, in these conditions, HGF-triggered cell proliferation does not contribute significantly to wound closure.

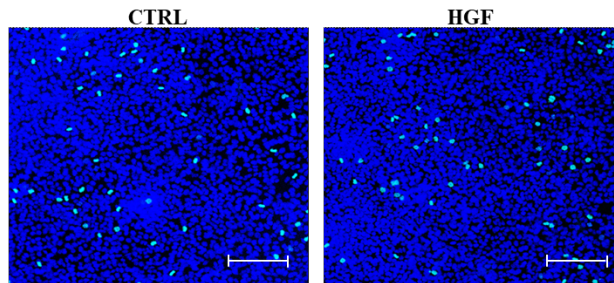
The reported values in Table 3 show that there is not a significant difference in the amount of pHH3⁺ cells between control and HGF treated cells, even in the confluent part of the culture dishes.

Therefore, these experiments demonstrate that the SUM(I) analysis as well as the count of pHH3⁺ cells does not reveal any increase of pHH3⁺ cell in the area of the wound in all samples considered. Furthermore, proliferation appears not responsible of NT2D1 cell collective migration. It is fair to consider that even in the areas far from the wound the number of pHH3⁺ cells as well as the SUM (I) of blue nuclear staining was not statistically significant. These data clearly indicate that the wound repair depends on a migratory effect of HGF on NT2D1, and that the cultural condition in which this experiment has been carried-out did not allow to underline the HGF- mediated NT2D1 cell proliferation, probably due to the over-confluence of the cells at the plating time.

PANEL A



PANEL B



PANEL C

Confocal analysis of the whole field in the wound areas				Confocal analysis of the wound area only (central part of the field)			
Table 1	SUM (I) green	SUM (I) blue	pHH3+ cells	Table 2	SUM (I) green	SUM (I) blue	pHH3+ cells
CTRL	1359 ± 300	63011 ± 2584	19 ± 2,8	CTRL	230,739 ± 25,037	20636 ± 1629	4 ± 0,4
HGF	1800 ± 265	65253 ± 4502	22 ± 1,1	HGF	308,278 ± 36,800	32167 ± 955	4,5 ± 0,6
p value	n.s.	n.s.	n.s.	p value	n.s.	P<0,001	n.s.

Confocal analysis of the areas far from the wound			
Table 3	SUM (I) green	SUM (I) blue	pHH3+ cells
CTRL	5733 ± 780	915604 ± 154953	53 ± 8
HGF	6559 ± 970	933214± 164504	67 ± 6
p value	n.s.	n.s.	n.s.

Figure 10: pHH3+ cells immunofluorescence in wound-healing assay of NT2D1 cells, cultured with or without HGF. (pHH3+ cells green, nuclei blue scale bar: 150 µm). Panel A: Maximum projection of representative optical

spatial series with step size of 1 μm recovered at the area of the wound. The dotted lines indicate the presumptive area of the wound, calculated at the beginning of the wound-healing assay. **Panel B.** Maximum projection of representative optical spatial series of the same samples of Panel A recovered in areas far from the wound. **Panel C:** Confocal microscopy quantitative analysis by Leica Confocal Software, of the SUM(I) of pHH3+ cells and nuclei. pHH3+ cells per field were also counted. All experiments were performed in triplicate and reported as mean \pm S.E.M.

4.2 c-Src is involved in HGF-dependent NT2D1 responses

4.2.1 Src inhibitor-1 does not affect cell viability

The c-MET/HGF system is a very intricate signalling, whose activation is responsible of a complex pathway activation cascade. Among the numerous proteins activated, c-Src represents one of the most intriguing ones. In light of this observation, we decided to start the investigation analysing possible c-Src activation after HGF treatment in NT2D1 cells. In this regard, we decided to use a pharmacological approach, using an inhibitor for this molecule, an ATP-competitor, called Src inhibitor-1. Dose response experiments were performed to highlight the better working dilution of Src inhibitor-1. Different concentrations of Src inhibitor-1 (1, 2.5, 5, 10 μM) were used for 48 hours. 10 μM of Src inhibitor-1 caused a significant increase in the percentage of cell death compared to the control condition ($p < 0,05$). For this reason, we decided to use this inhibitor at 5 μM , a concentration that can be considered not toxic also after 72 hours of treatment (Figure 11, panel I). As an additional check, “trypan blue exclusion test” was performed, demonstrating that the concentration of 5 μM Src inhibitor-1 does not cause cell death in this cellular line (data not shown).

This concentration was tested also with immunofluorescence analysis using an antibody against cleaved caspase3, demonstrating that the number of cleaved caspase3 positive cells was not statistically different between treated cells and control condition (Figure 11, panel II).

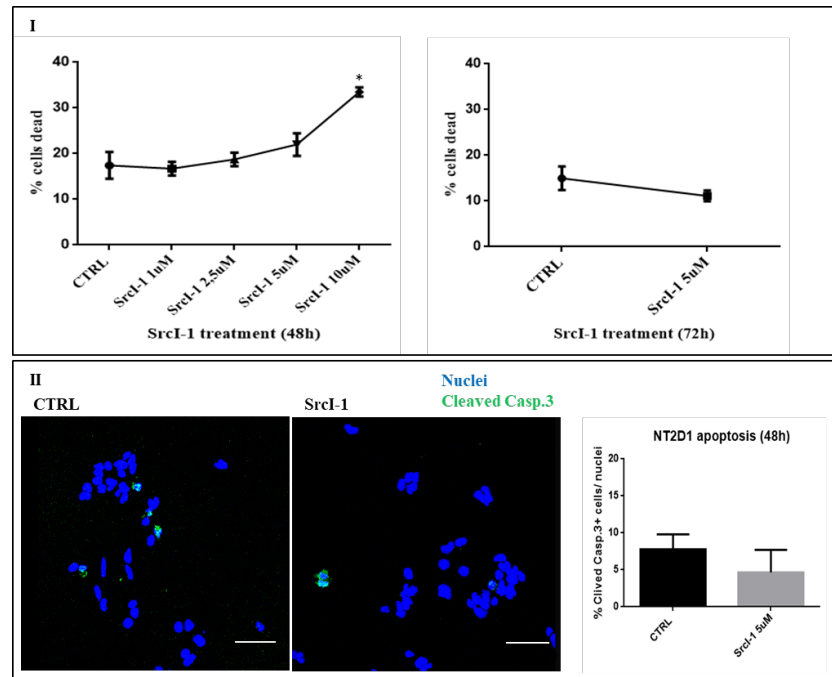


Figure 11: I) Cell death FACS analysis on NT2D1 cells. On the left: graphical representation of the percentage of dead cells obtained culturing NT2D1 cells with different concentration of Src inhibitor-1 for 48h (* $p < 0,05$). On the right: graphical representation of the percentage of dead cells obtained culturing for 72h NT2D1 cells with 5 μ M Src inhibitor-1 ($p = n.s.$). **II)** on the left: representative images of cleaved caspase3 immunofluorescence on cells treated with 5 μ M Src inhibitor-1 for 48h (scale bar 80 μ M). On the right: quantitative analysis, by Leica Confocal analysis of the number/field of cleaved caspase3 positive cells (FITC/green signal) normalized versus and the number of nuclei (TOPRO-3/blue signal) ($p = n.s.$).

4.2.2 c-Src is involved in HGF-dependent NT2D1 proliferation

As previously mentioned, HGF specifically activates its receptor c-MET on NT2D1 cells, resulting in an increase of proliferation rate after 48h of culture. To investigate the role of c-Src in HGF-dependent c-MET activated cell proliferation, we performed proliferation assay using Src inhibitor-1. On the basis of the mentioned previous work (102), NT2D1 cells were cultured for 48h in basal condition or with the following treatments: Src

inhibitor-1, HGF, or HGF+ Src inhibitor-1 (Figure 12). Then cells were detached and counted. As expected HGF administration induced a significant increase of cell number with respect to control samples ($1,2 \pm 0,06$ vs 1 ± 0.04 , respectively; $p < 0.001$).

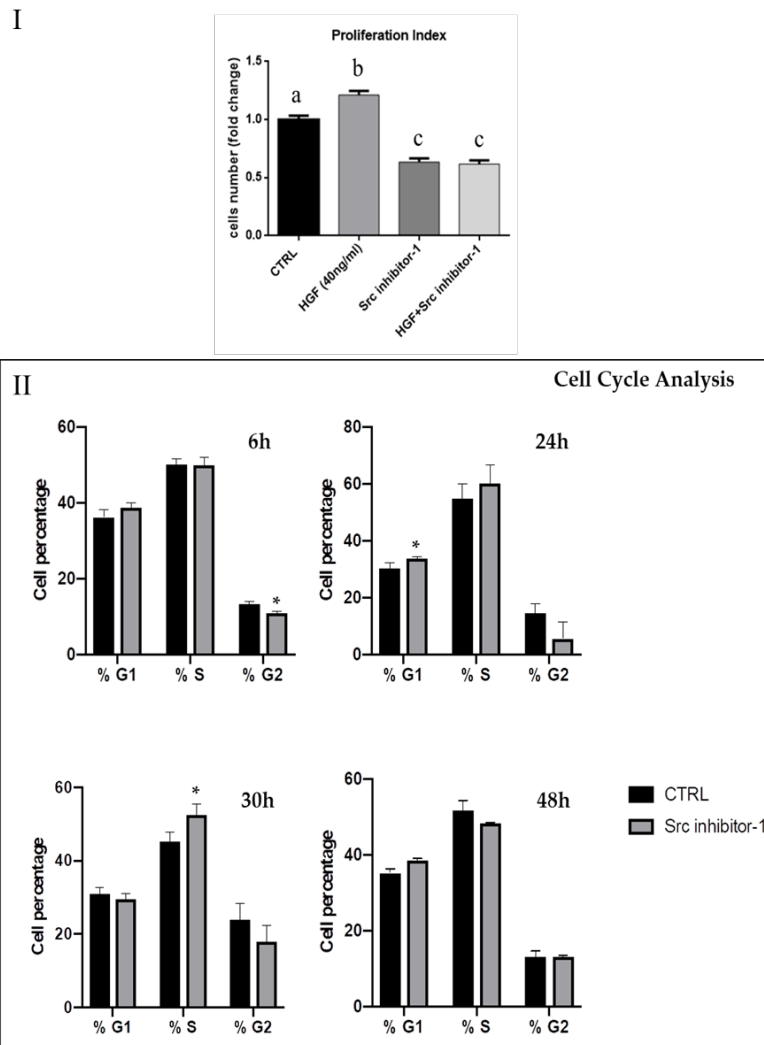


Figure 12: Effect of Src Inhibitor-1 on NT2D1 cell proliferation induced by HGF. I) Graphical representation of the number of NT2D1 cell cultured for

48h in 2% FBS DMEM (CTRL), or with: HGF, Src inhibitor-1, or their combination. HGF treatment shows a significant increase of cell number (b vs a; $p < 0,001$). Using the inhibitor, with or without HGF, we observed a significant reduction of cell proliferation compared to the HGF (c vs b; $p < 0,001$), and to the control condition (c vs a; $p < 0,001$). Four independent experiments were performed at least in triplicate. Results were expressed in fold change and the control was considered as 1 (\pm S.E.M.). **II**) Table illustrating the results of cell cycle analysis on NT2D1 cell cultured for 6, 24, 30 and 48h with or without Src inhibitor-1 (* vs the respective control $p < 0,05$).

Using HGF+ Src inhibitor-1, we observed that the treatment completely abrogates the HGF induced proliferation in NT2D1 cells ($0,7 \pm 0,04$ vs $1 \pm 0,04$ respectively; $p < 0,001$). Surprisingly, using Src inhibitor-1 alone determined a proliferation rate significantly different compared to the control ($0,7 \pm 0,04$ vs $1 \pm 0,04$ respectively; $p < 0,001$). To better characterize this phenomenon, we performed cell cycle analyses, which revealed that Src inhibitor-1 administered alone, causes a significant decrease of cells in G2 phase after 6 hours of culture, a significant increase of cells in G1 phase after 24 hours of culture and a subsequent significant increase of cells in S phase after 30 hours of culture (Figure 12; panel II). These results indicate that Src inhibitor-1 causes a slight cell cycle slowdown, when administered alone. Moreover, in light of these results, we can speculate that c-Src regulates NT2D1 cell proliferation both in HGF-dependent and HGF-independent way.

4.2.3 c-Src is specifically involved in HGF-dependent NT2D1 chemo-attraction

To deeper investigate the molecular effectors involved in a migration process, we decided to test if c-Src is required for HGF-mediated chemo-attraction of NT2D1 cells. We performed the above-mentioned chemotaxis assay, using Src inhibitor-1 (Figure 13). We observed that this inhibitor administered alone did not affect migration rate with respect to basal condition (1.4 ± 0.2 vs 1 ± 0.09 respectively; $p = n.s.$), while, as expected, HGF induced the chemotactic migration of NT2D1 cells (2 ± 0.16 vs $1 \pm 0,09$

respectively; $p < 0,001$). But, in detail, the treatment of cells with Src inhibitor-1 in the upper chamber of the trans-well apparatus significantly reverted the migratory effect exerted by HGF added in the lower chamber ($1,2 \pm 0,13$ vs $2 \pm 0,16$ respectively; $p < 0.01$). Thanks to these results, we can state that c-Src is involved in the positive regulation of this phenomenon.

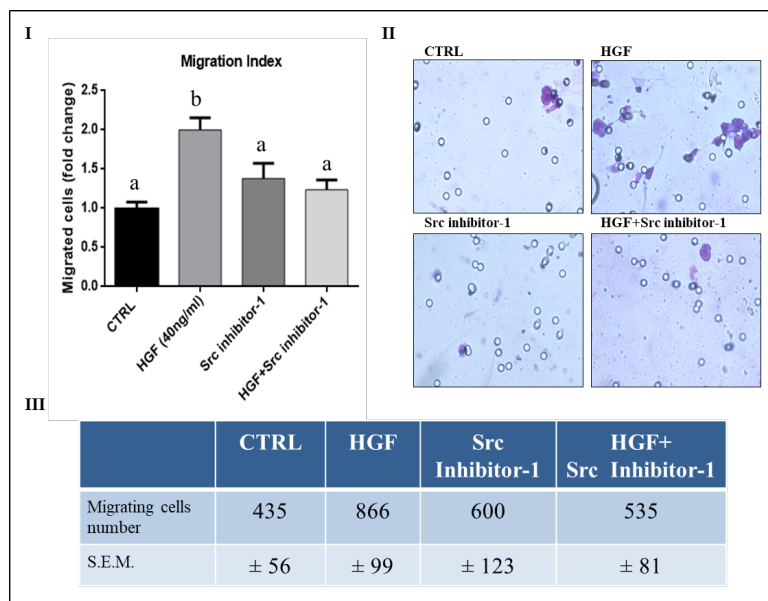


Figure 13: Effect of Src inhibitor-1 on NT2D1 chemo-attraction: I) Graphical representation of the amount of chemo-attracted NT2D1 cells. A significant increase of migrated cells using HGF was observed (b vs a; $p < 0.001$). The use of Src inhibitor -1 in combination with HGF abrogates the effect induced by HGF. Control condition was arbitrarily considered as 1, and the values were calculated as “fold change” compared with control. **II)** Representative images of NT2D1 migration, obtained with Diff quick staining. Images were recorded at 40X magnification. **III)** Table illustrating the number of migrating cells/filter in all the experimental conditions reported in the respective “fold change” graph (b vs a; $p < 0.001$).

4.2.4 c-Src is involved in HGF-induced collective migration

It is well known that HGF binding activates c-MET, resulting into tyrosine residues phosphorylation. Active c-MET recruits signaling

effectors that activate protein kinases, such as c-Src, ultimately leading to cell migration (59). To investigate whether HGF-induced wound migration is dependent on c-Src recruitment,

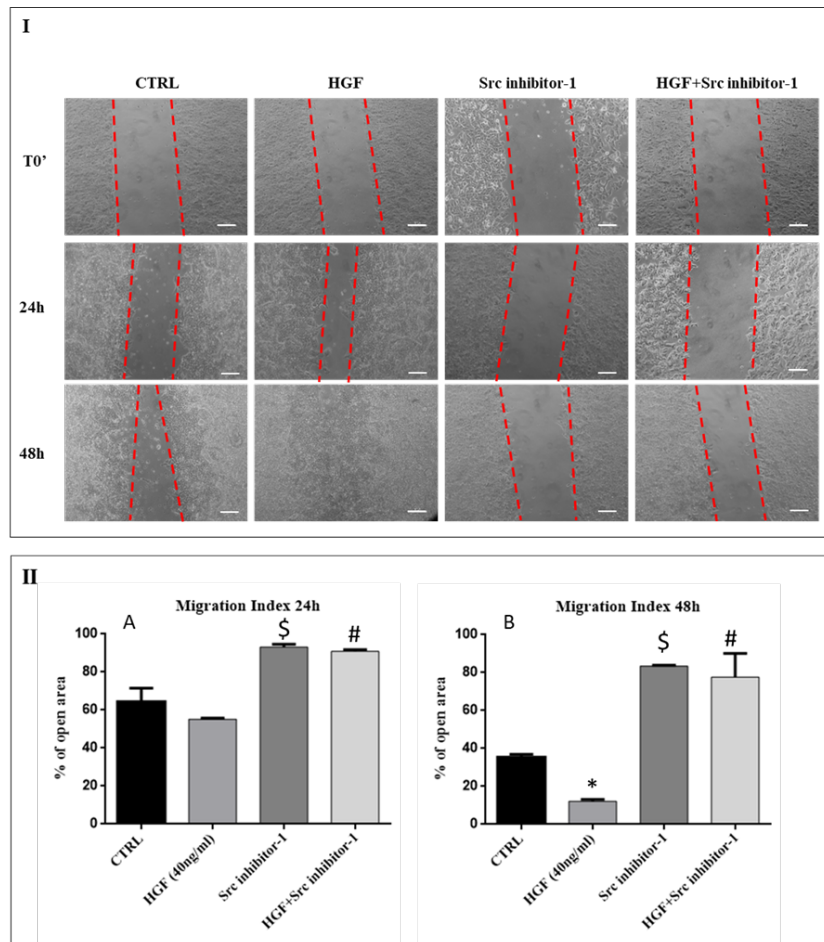


Figure 14: Effect of Src Inhibitor-1 on NT2D1 cell collective migration. Three independent experiments were performed at least in quadruplicate. **I)** Representative phase contrast images of wound healing assay recovered immediately after insert removal (T0) and 24h and 48h after wounding. Images were photographed at 10X magnification (scale bar: 100 μ m). **II)** Quantitative analysis of wound closure after 24h (A) and 48h (B). Data are expressed as the mean percentage of residual open area compared to the respective cell-free

surface recovered at T0. At 24h the decrease of open area in HGF treated cells was not statistically significant compared with control condition, but the closure was almost complete at 48h (* $p < 0.001$). Src inhibitor-1 in combination with HGF both at 24h (# $p < 0.01$) and 48 h (# $p < 0.001$) abrogated the migratory effect induced by HGF. Src inhibitor-1 alone was also able to inhibit the collective migration of the cells cultured for 24 h (\$ $p < 0.05$), and 48 h (\$ $p < 0.001$).

NT2D1 cells were incubated with medium alone or with HGF in the presence or not of Src inhibitor-1.

The results showed collective cell migration more evident in HGF-exposed NT2D1 cells after 48h treatment with respect to constitutive migration observed in the control condition (Figure 14).

More in detail, after 24h of culture the open residual area of samples treated with Src inhibitor-1 alone showed values similar to its own T0 ($93.1\% \pm 1.5$) and, therefore, significantly higher compared with control condition ($64.4\% \pm 7.1$) and HGF treated wells ($55.2\% \pm 0.6$). After 48h, these areas remained almost unchanged ($83.5\% \pm 0.3$) with respect to 24h, whereas the open residual area of control samples and HGF treated wells decreased ($35.4\% \pm 1.5$ and $12.2\% \pm 1$ respectively). The inhibition of collective cell migration in the presence of Src inhibitor-1 alone clearly indicates the involvement of this adaptor-protein in constitutive collective migration of NT2D1 cells, even if further investigations are needed to clarify this point.

Src inhibitor-1 administration reduces also the enhanced collective migration induced by HGF. The values of open residual area of HGF+ Src inhibitor-1 treated wells were significantly higher, compared with HGF treated wells, already after 24h of culture ($90.9\% \pm 0.9$ vs $55.2\% \pm 0.6$ respectively). This difference was even more significant after 48h of culture ($77.6\% \pm 12$ vs $12.2\% \pm 1$ respectively) (Figure 14).

4.2.5 c-Src is involved in HGF-dependent cells invasion

Our previous work demonstrated that HGF is able to induce higher invasive capabilities in NT2D1 cell line (102). To better understand the mechanism involved in this biological response, we

performed invasion assays, using the Src inhibitor-1. As shown in Figure 15, we confirm that HGF treatment significantly modulates the invading capability of NT2D1 cells ($2,2 \pm 0,3$ vs $1 \pm 0,16$ respectively). On the other hand, when Src inhibitor-1 was used in combination with HGF, the number of invading cells reverts to control condition ($1 \pm 0,21$ vs $1 \pm 0,16$ respectively; $p=n.s.$). Notably, we also found that Src inhibitor-1 alone significantly increases NT2D1 cell invasiveness compared to the control condition ($1,75 \pm 0,4$ vs $1 \pm 0,16$ respectively; $p<0,05$) and the value results similar to HGF administration ($1,75 \pm 0,4$ vs $2,2 \pm 0,3$; $p=n.s.$). This result is relevant and deserves further investigation to fully characterize the mechanism underlying it. Taken together, these findings demonstrate that c-Src is involved in the regulation of NT2D1 cell invasiveness, using both HGF-dependent and HGF-independent pathways.

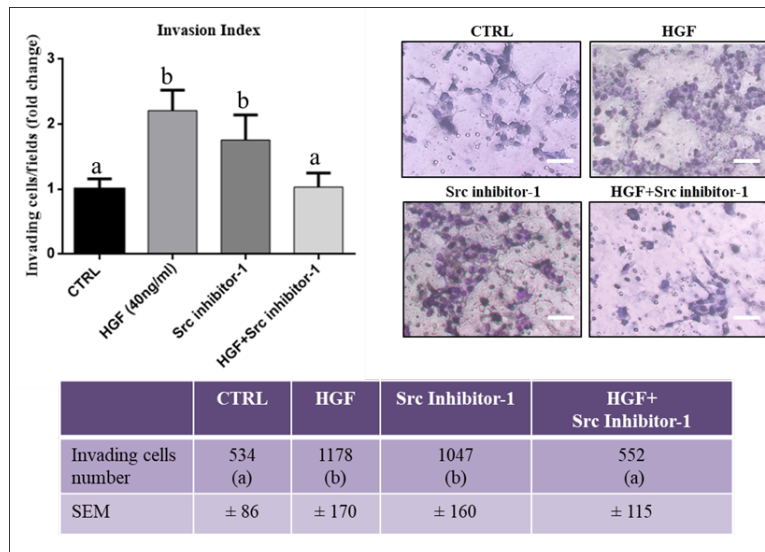


Figure 15: Effect of Src Inhibitor-1 on NT2D1 cell invading capability: Invasion assay was performed using filters coated with GFR Matrigel. The filters were analyzed by optical microscope and images were recovered at 10X magnification. Three independent experiments were performed at least in triplicate. Left panel: Quantitative analysis of invading cells. The results are

expressed as fold change (\pm S.E.M.) and the control condition is considered as 1. HGF and Src inhibitor-1 alone induced both a statistically significant increase in NT2D1 cell invasion with respect to the control (b vs a; $p < 0.05$). The treatment of HGF+ Src inhibitor-1, abrogated this effect. Right panel: Representative phase contrast images of the different culture conditions. Images demonstrate a higher invasiveness behaviour of cells treated with HGF or Src inhibitor-1 alone compared with HGF+ Src inhibitor-1 condition. The table in the lower panel illustrates the number of invading cells/filter in all the experimental conditions reported in the respective “fold change” graph (b vs a; $p < 0.05$).

4.2.6 Phospho-c-Src detection after HGF administration

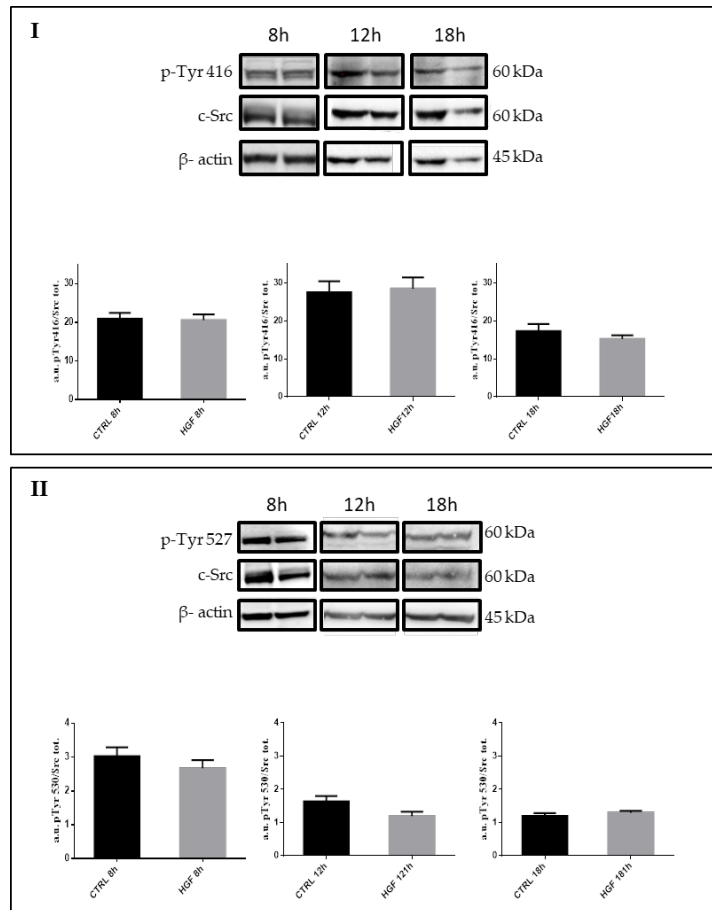


Figure 16: c-Src expression and phosphorylation of NT2D1 cells exposed to HGF. I) Western blot analysis of c-Src Phospho Tyr 416, total c-Src protein, and β - actin in NT2D1 cell lines cultured for 8h, 12h and 18h, with or without HGF. In the lower part of the panel the densitometric analyses of c-Src phospho Tyr 416 bands normalized versus total c-Src/ β -actin are shown. **II)** Western blot analysis of c-Src phospho Tyr 527, total c-Src protein, and β - actin in NT2D1 cell lines cultured for 8h, 12h and 18h with or without HGF. In the lower part of the panel the densitometric analyses of c-Src phospho Tyr 527 bands normalized versus total c-Src/ β -actin are shown.

It is known that c-MET phosphorylation determines several biological responses, and in a previous work we demonstrated that HGF triggers c-MET phosphorylation 6h after treatment (102). To analyze whether c-Src phosphorylation changes after HGF administration, we performed western blot analyses at different culture times (8, 12 and 18 hours) (Figure 16). c-Src activation is peculiar, since it is regulated by the phosphorylation of two key tyrosines: Tyr527 that needs to be dephosphorylated to allow c-Src activation that is in turn due to the autophosphorylation of Tyr416. Therefore, we performed western blot analyses using anti-c-Src Phospho Tyr 416, and anti-c-Src Phospho-Tyr 527, both normalized versus total c-Src/ β actin. Surprisingly, we did not observe significant modulation of c-Src active or inactive isoform due to HGF administration. Notably, fluctuation of both isoforms is reportable during culture time, indicating that a constitutive turnover of activation/inactivation occurs.

4.2.7 Immunofluorescence analysis of the active form of c-Src (phospho Tyr 416)

To describe the distribution of the active form of c-Src in our experimental conditions, we performed immunofluorescence analyses using anti-c-Src (phospho Tyr 416). Interestingly, we found that, after HGF administration the active form of c-Src appears mainly localized in the nucleus, even if the cytoplasmic/membrane localization does not disappear in the HGF treated samples (Figure 17). This result is very interesting and shed new light in the modality of action of HGF-dependent c-Src

activation. The presence of c-Src in the nuclear compartment of normal and cancer cells was already reported by some groups (104-106), even if the relevance of this phenomenon for cancer cell aggressive behaviour gave, so far, discordant results. In our experimental model this observation triggers the intriguing hypothesis that HGF-mediated c-Src activation causes rapidly the modification of gene expression via the translocation of the active form of c-Src in the nucleus of NT2D1 cells.

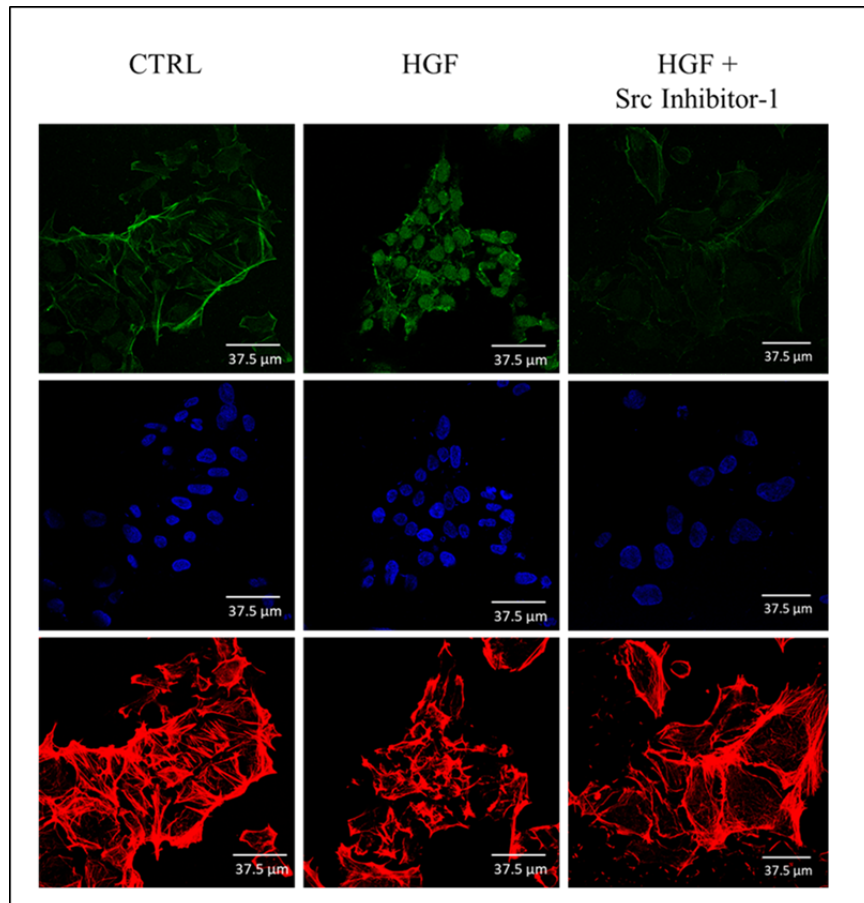


Figure 17: Confocal microscopy analysis of c-Src phospho Tyr416 distribution-pattern. Immunofluorescence analyses of c-Src phospho Tyr416

(FITC, green signal) in NT2D1 cells cultured with or without HGF and Src Inhibitor-1. Actin cytoskeleton (Rhodamin phalloidin, red signal) and nuclei staining (TOPRO-3, blue signal) are also reported in the figure. The nuclear translocation of c-Src phospho Tyr416 after HGF administration is well evident. The treatment with Src Inhibitor-1 prevents this phenomenon.

4.3. PI3K/AKT involvement in NT2D1 cellular responses

4.3.1 PI3K/AKT is active in NT2D1 cells and LY294002 does not affect cell viability

It is well known that HGF/c-MET system is able to induce, PI3K/AKT pathway responses (59). To test if the biological responses of NT2D1 cells observed in our previous work (102) (*i.e. proliferation, migration, invasion*) are dependent also on this pathway, we treated NT2D1 cells with HGF and with a PI3K inhibitor (LY294002).

Firstly, to identify the not toxic dose in NT2D1 cell lines, we performed cell death FACS analysis with different LY294002 concentrations (1, 5, 10, 15 μ M) for 48 hours. These experiments demonstrated that there is not statistically significant difference in live cells percentage with respect to control condition when the inhibitor is used at 1 and 5 μ M (about $106\% \pm 5$ for 1 μ M and $99\% \pm 2$ for 5 μ M. Control is reported as 100%). Starting from 10 μ M, the inhibitor causes a significant decrease in cell viability compared to the control condition (about $80\% \pm 2$ for 10 μ M and $55\% \pm 6$ for 15 μ M. Control is reported as 100%) (Figure 18, panel I). “Trypan blue exclusion test” was also performed and confirm that the concentration of 5 μ M LY294002 does not cause cell death in this cell line (data not shown).

Western blot analysis of p-AKT and total AKT in NT2D1 cell lines cultured in four different experimental conditions (CTRL, HGF, LY294002 and HGF+LY294002) were performed. Densitometric analysis of the bands demonstrated that HGF alone significantly increase the phosphorylation of AKT in the activator site (Ser 473) after 30 minutes of treatment. 5 μ M LY294002, alone or in combination with HGF, is able to inhibit significantly this cellular

response and the values result similar to the control (Figure 18, panel II).

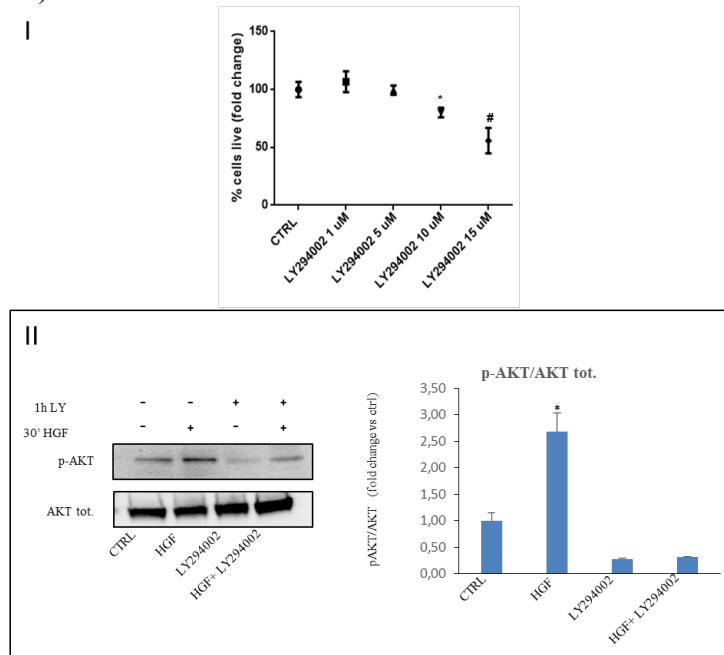


Figure 18: I) Cell death FACS analysis on NT2D1 cells. Graphical representation of the percentage of live cells (in fold change) obtained culturing NT2D1 cells with different concentration of LY294002 for 48h (* $p < 0,05$; # $p = 0,001$). **II)** Western blot analysis of p-AKT and total AKT in NT2D1 cell lines cultured with LY294002 and with HGF. On the left: representative images of p-AKT and total AKT bands are shown. On the right: densitometric analysis of pAKT/AKT (* $p < 0,05$).

4.3.2 HGF-dependent NT2D1 proliferation is dependent on PI3K/AKT

As previously demonstrated (102), HGF specifically determines c-MET activation, which leads to significant NT2D1 proliferation increase after 48h of culture. To test if PI3K/AKT is involved in this response, NT2D1 cells were cultured for 48h in basal condition (CTRL) or treated with LY294002, HGF or HGF+ LY294002 (Figure 19). Then, cells were detached and counted.

Using LY294002 alone, we observed a proliferation rate not significantly different from control ($0,98 \pm 0,07$ vs $1 \pm 0,06$ respectively; $p=n.s.$). As expected, HGF induced a significant increase of cell number after 48h of culture with respect to the control condition ($1,36 \pm 0,06$ vs $1 \pm 0,06$ respectively; $p<0,001$). On the contrary, using HGF+ LY294002, we observed that the treatment completely abrogates the HGF induced proliferation of NT2D1 (proliferation rate was similar to control value ($0,98 \pm 0,06$ vs $1 \pm 0,06$ respectively; $p=n.s.$). Taken together, our results demonstrate that PI3K is involved in HGF-dependent proliferation of NT2D1 cells.

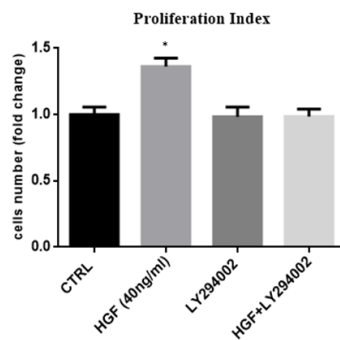


Figure 19: Effect of LY294002 on NT2D1 cell proliferation induced by HGF. Graphical representation of the number of NT2D1 cell cultured for 48h in 2% FBS DMEM (CTRL), or with: HGF, Src inhibitor-1, or their combination. HGF determined higher proliferation rate (* $p<0,001$). Results were expressed in fold change and the control was considered as 1 (\pm S.E.M.). Three independent experiments were performed at least in triplicate.

4.3.3 PI3/AKT pathway is involved in HGF-dependent NT2D1 migration

We have established that HGF acts as a chemo-attractant for NT2D1. In fact, HGF is able to increase cell migration evaluated by Boyden chambers migration assays (102). In this elaborate, as reported above, we have demonstrated that this migration is c-MET specific and that c-Src is involved in this process. Literature data reveals a strong correlation between c-Src and PI3K/AKT pathways, in turn activated by c-MET. In this work we analyse the possible involvement of PI3K/AKT pathway in HGF-induced chemotaxis. We performed migration experiments, as above mentioned in materials and methods section, using PI3K inhibitors, LY294002. The inhibitor alone did not affect migration rate with respect to the control condition ($1,1 \pm 0,08$ vs $1 \pm 0,1$ respectively;

p=n.s.). As shown in figure 20, as expected, migration significantly increases in presence of HGF respect to the control ($1,8 \pm 0,2$ vs $1 + 0,1$ respectively; $p < 0,001$). On the contrary, the treatment of cells with LY294002 significantly reduce the migratory effect induced by HGF ($1,2 \pm 0,07$ vs $1,8 \pm 0,2$ respectively; $p < 0,001$). Taken together, these results confirm that NT2D1 chemotaxis is HGF-dependent and that PI3K/AKT pathway is involved in this phenomenon.

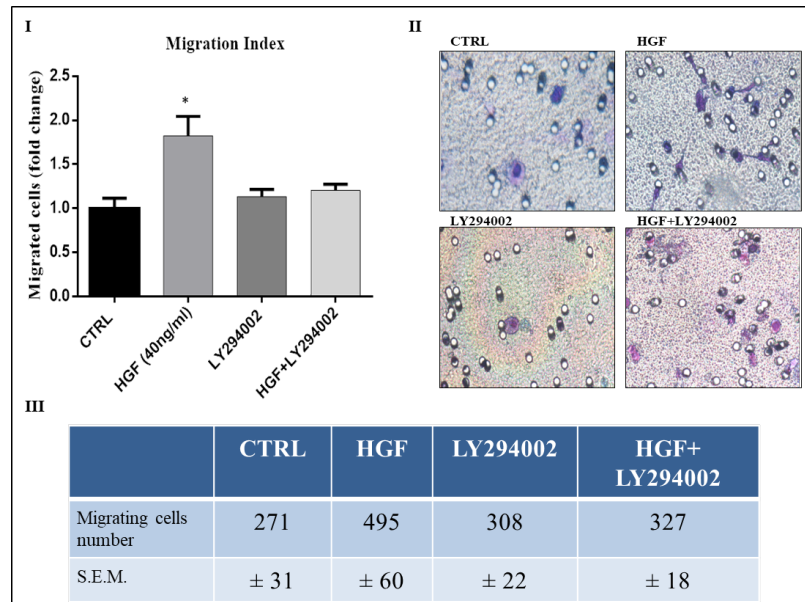


Figure 20: Effect of LY294002 on cell migration: I) Graphical representation of the amount of chemo-attracted NT2D1 cells. The use of LY294002 in combination with HGF abrogates the effect induced by HGF. Control condition was arbitrarily considered as 1, and the values were calculated as “fold change” compared to the control. **II)** Representative images of NT2D1 migration obtained with Diff quick staining. Images were recorded at 40X magnification. **III)** Table illustrating the number of migrating cells/filter in all the experimental conditions reported in the respective “fold change” graph (* $p < 0,001$).

4.3.4 PI3K/AKT pathway is involved in HGF-induced collective migration

HGF binding activates c-MET, which is able to induce collective migration in NT2D1 cells as we previously demonstrate (102). In order to investigate if this phenomenon is also driven by PI3K pathway, we performed wound healing assay, as described in material and methods section, in the following experimental conditions: control condition, HGF, LY294002 alone or HGF + LY294002.

As expected, HGF administration determined an evident collective cell migration both at 24h and at 48h of treatment (Figure 21). More in detail, in these experiments we measured the open area of each sample at T0, considered as 100%. After 24 and 48 h, we measured the open residual area for each condition.

As shown in figure 21, after 24h of culture, the decrease of the open residual area in HGF treated cells appears not statistically significant compared to the control condition (55% vs 64,41%). On the other hand, after 48h of treatments, the open residual area of HGF treated cells results significantly reduced (12%) and the closure of the wound is almost complete respect to all condition considered (approximately 85% in LY294002 alone or with HGF and 35% the control). Samples treated with LY294002 alone both at 24h (90%) and 48h (85%) were similar to their relative T0 (100%).

Sample treated with HGF+ LY294002 both at 24 and 48h also shown an open residual area not significantly different from their T0 (90% 24h and 85% 48h) (Figure 21).

The decrease of cell migration in presence of LY294002 inhibitor alone clearly indicates the involvement of this pathway in constitutive collective migration of the cells. Furthermore, the migratory phenomenon increased in presence of HGF is reduced also with HGF+ LY294002, suggesting that PI3K/AKT signalling is required not only for endogenous migration, but also for increased HGF-induced migration.

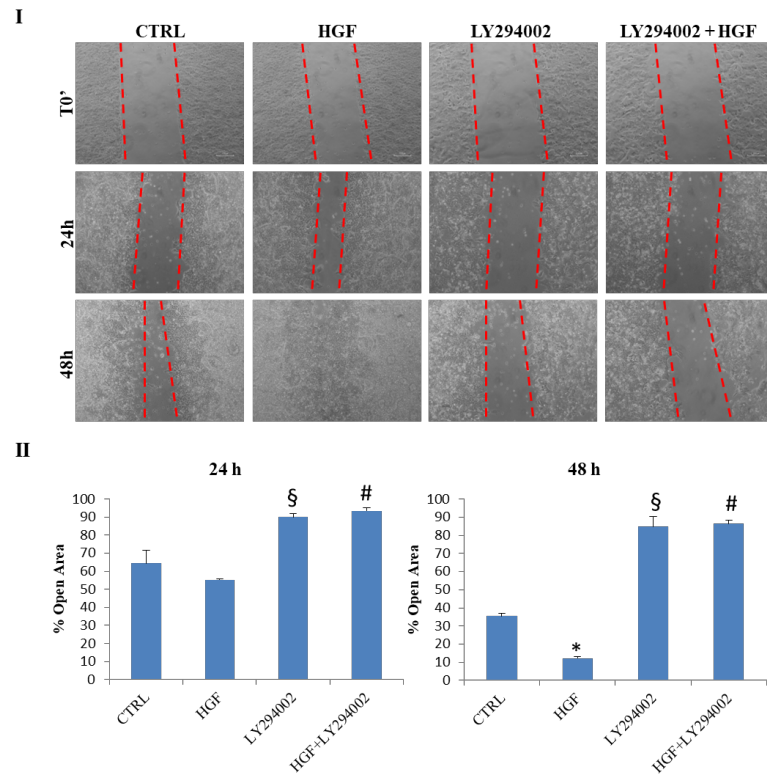


Figure 21: Effect of LY294002 on NT2D1 cell collective migration. I) Representative phase contrast images of wound healing assay recovered immediately after insert removal (T0) and 24h and 48h after wounding. Images were photographed at 10X magnification (scale bar: 100 μ m). **II)** Quantitative analysis of wound closure after 24h (A) and 48h (B). Data are expressed as the mean percentage of residual open area compared with the respective T0 condition. At 24h the decrease of open area in HGF treated cells was not statistically significant compared with control condition, but the closure was almost complete at 48h (* p <0.001). LY294002 in combination with HGF both at 24h (# p <0.01) and 48h (# p <0.001) abrogated the migratory effect induced by HGF. LY294002 alone was also able to inhibit the collective migration of the cells cultured for 24h (\$ p <0.05) and 48h (\$ p <0.001). Three independent experiments were performed. Each experiment was performed in triplicate.

4.3.5 PI3K is involved in HGF-dependent cells invasion

To better understand the mechanism involved in NT2D1 invasion modulated by HGF as we previously demonstrated (102), we performed experiments using Matrigel coated Transwell to evaluate the role of PI3K in this aspect of tumorigenesis. Cells were seeded on Matrigel layer and then they were treated with HGF or PI3K inhibitor, LY294002, as schematized in Figure 22. Results confirm our previous data, demonstrating that HGF treatment specifically modulates the capability of invasion in NT2D1 cells in a c-MET-specific way, in fact HGF administration increases invading cells number in a statistically significant difference with respect to the control condition ($2,0 \pm 0,27$ vs $1 \pm 0,3$ respectively; $p < 0,05$). We also observed that LY294002 alone significantly increases invasion behaviour of NT2D1 cells with respect to the control condition ($2,37 \pm 0,2$ vs $1 \pm 0,3$ respectively; $p < 0,05$) resulting in values similar to HGF condition ($2,0 \pm 0,27$ vs $2,37 \pm 0,2$; $p = n.s.$). On the contrary, when LY294002 was used in combination with HGF, the number of invading cells is closely related to the control condition ($1 \pm 0,26$ vs $1 \pm 0,3$ respectively; $p = n.s.$).

Taken together, these results demonstrate a crucial role of PI3K/AKT pathway in HGF-dependent NT2D1 cells invasion. However, inhibition of PI3K has a positive effect on NT2D1 cells invasion. A probable explanation of this result is that NT2D1 endogenous capability to invade extracellular matrix is microenvironment-dependent. Starting from this aspect, which it requires further study for its understanding, we can speculate that cytoskeleton remodelling can occur in presence of LY294002. In our opinion, this phenomenon is a proof of the important role involved by microenvironment and the presence or the absence of HGF are a crucial point for the different biological responses in NT2D1 cell line.

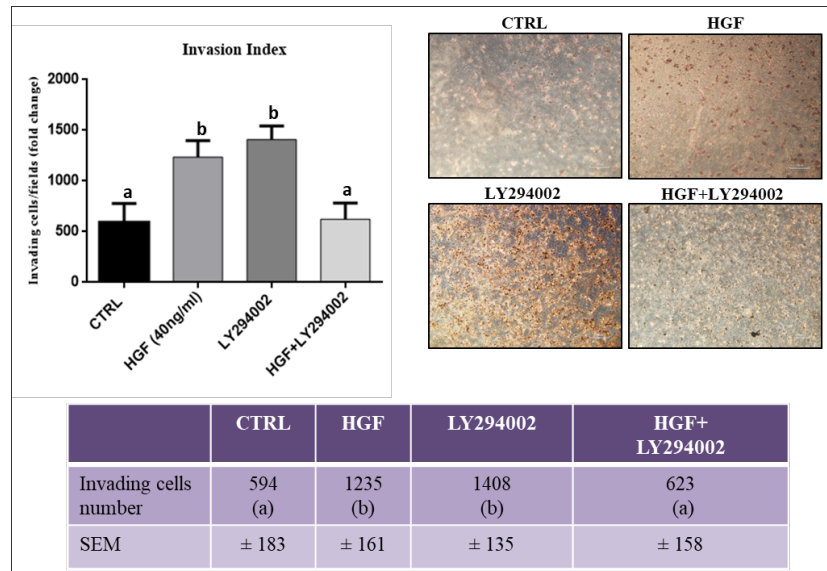


Figure 22: Effect of LY294002 on NT2D1 cell invading capability using trans-well coated with GFR Matrigel. Filters were analyzed by optical microscope and images were recovered at 10X magnification. Three independent experiments were performed at least in triplicate. Left panel: Quantitative analysis of invading cells. Results are expressed as fold change (\pm S.E.M.) and the control condition is considered as 1 (b vs a; $p < 0.05$). Right panel: representative phase contrast images of different culture. Lower panel: the table illustrates the number of invading cells/filter in all the experimental condition.

4.3.6 HGF induced NT2D1 morphological modification through PI3K/AKT

To study at the highest definition possible whether HGF/c-MET pathway activation could modify NT2D1 cell shape, membrane surface morphology and activity, samples were analyzed by Scanning Electron Microscopy (SEM). Cells were treated for 24h with HGF and analysed by SEM, as described in the material and methods section.

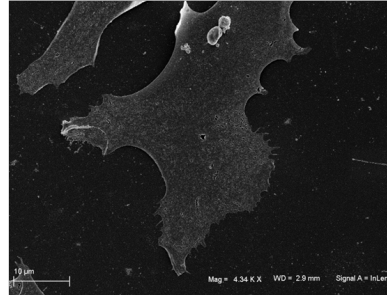
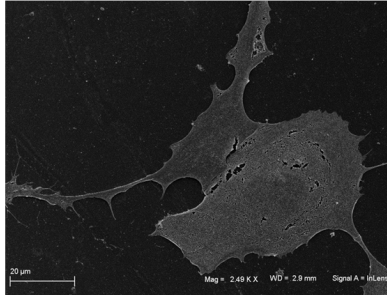
This analysis reveals that HGF treated cells thoroughly modify their shape appearing stretched and strongly characterized by the presence of membrane expansions, such as microvilli-like structures, filopodia, and lamellipodia. Moreover, SEM analysis

demonstrates that HGF is able to induce microvesicles formation on the cell surfaces. As previously mentioned, this experimental condition also determines the formation of filopodia and lamellipodia, confirming the migratory attitude induced in these cell line by HGF administration. On the contrary, in the control condition the situation appears very different. Control has smooth membrane surface and membrane protrusions appear absent (Figure 23).

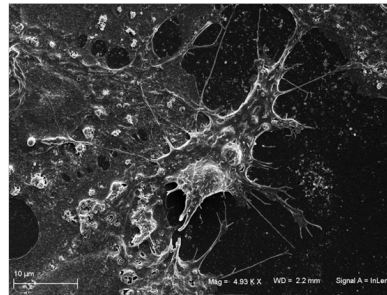
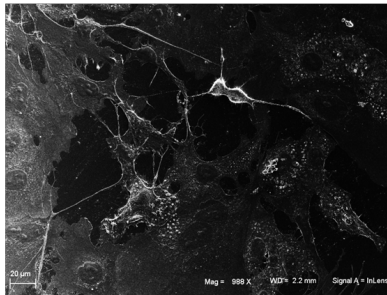
As previously described, in NT2D1 cells we observed that the PI3K/AKT system induces higher aggressive capabilities when related with the control condition. SEM analysis showed that the co-administration of LY294002 with HGF is able to revert the membrane appearance to the control condition, while LY294002 alone determines an intermediate situation between the control condition and HGF treated cells (Figure 23). In fact, LY294002 administration alone induces remodeling of the cell surfaces similar, in part, to the effect induced by HGF administration.

The mechanism of cell movement is of utmost relevance for the metastasis process. Cells undergo a rearrangement of cytoskeleton in the leading edge, which lead to formation of filopodia and lamellipodia structures. This result is in line with results previously described, where invasion assay demonstrated that LY294002 alone determined higher aggressive capabilities in this cell line. Also in this case, the explanation may be that this cell line is heavily affected by the microenvironment and the cellular responses are microenvironment-dependent.

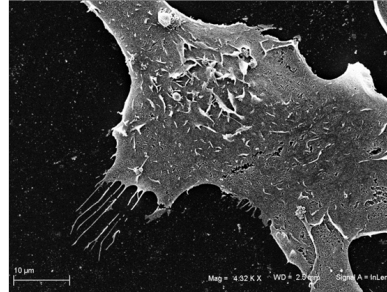
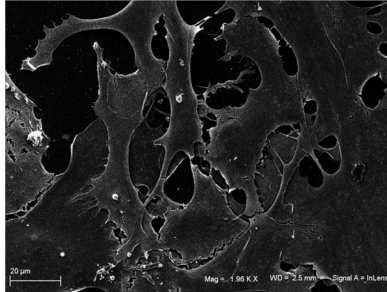
CTRL



HGF



LY294002



HGF + LY294002

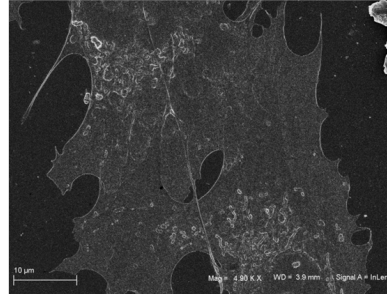
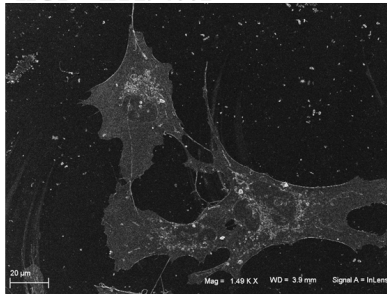


Figure 23: Scanning Electron Microscopy Analysis. On the right, representative images of SEM of NT2D1 treated cells for 24 hours with HGF, LY294002 and HGF+LY294002. On the left, scale bar 20 μm , while, on the right, high magnification with a scale bar 10 μm .

4.4 Link between c-Src and PI3K/AKT

4.4.1 Relation between PI3K/AKT and c-Src proteins

We demonstrated that NT2D1 cellular responses result in an involvement of c-Src protein, herein described. Other evidences here reported demonstrate that also PI3K/AKT pathway is implicated in the NT2D1 HGF-dependent effects. Literature data shows a strong correlation between c-Src and PI3K/AKT in other systems. To investigate if also in this cell line these two pathways are strictly correlated, we performed western blot analysis. Cells were treated with Src inhibitor-1 (also called SKI-1) for 15 and 60 minutes and protein extracts were analysed. The eventual inhibition of PI3K/AKT pathway was tested. Preliminary results show a reduction of AKT phosphorylation, and a consequent reduction of its activation, using c-Src inhibitor starting from 15 minutes in correlation with the control condition. This pilot experiment leads us to hypothesize in a close correlation between these two signalling and that c-Src is responsible for the activation downstream of PI3K/AKT in NT2D1 cells.

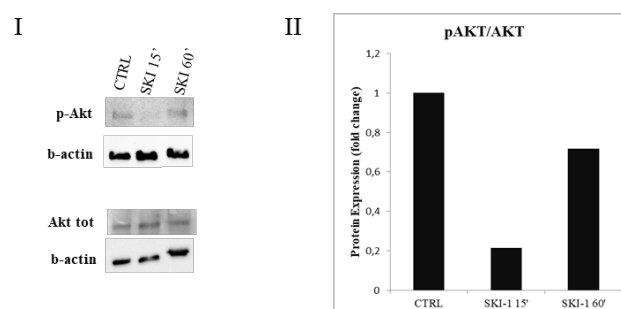


Figure 24: Preliminary data. I) Representative images of p-AKT and total AKT bands, both normalized with β -actin. II) Graphical representation of Western Blot analysis of samples treated with Src inhibitor-1 (SKI-1) for 15 and

60 minutes in DMEM 2% FBS. Results are expressed in fold change and the control was considered as 1.

4.4.2 Cytoskeletal remodeling HGF-dependent in NT2D1 cells

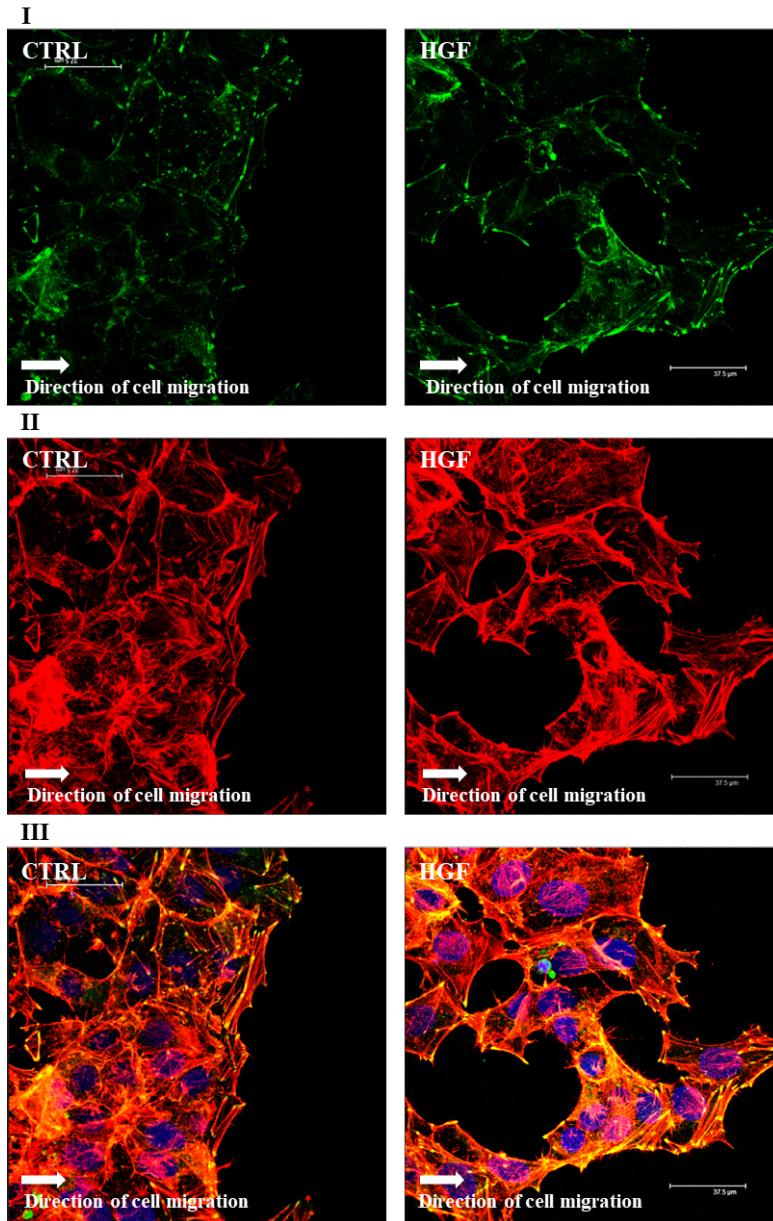
We observed and described in NT2D1 cells an increase in migration and invasion rate after HGF treatment. To better understand the morphological modification that are associated with migratory and invasive phenotype we focused our attention on cytoskeletal modifications that occur in this cell line which are responsible of cell motility. We performed wound healing assay on cells treated with HGF, Src inhibitor-1 and LY29002 (both inhibitors alone or in combination with HGF) and after 24h we analyzed by confocal microscopy vinculin and actin at front of migration.

As shown in Figure 25, HGF treatment on NT2D1 cells, determined clear actin/vinculin cytoskeletal changes. Cells appear more detached from each other with a major actin stress fibres formation, especially in the leading edge of the wound. Vinculin is present both in control and in HGF treated samples. However, its distribution is different in fact it is localized especially in the leading edge of the cellular membrane in HGF samples (Figure 25) while in the control samples vinculin appears more localized in the cell-cell contact and in internal compartment of the cytoplasm and less in the leading edge. Co-localization analysis of actin and vinculin indicate the presence of focal adhesion structures. These structures are clearly evident in membrane protrusion at leading edge of HGF treated cells (Figure 25). This suggests that at front of migration new focal adhesion formation, request for cell migration, occurs.

Taken together these results reflect and confirm the greatest ability of HGF treated cells to repair the wound already in the first 24 hours with respect to control cells as we demonstrated in this work (Figure 9).

Using LY294002 and Src inhibitor-1, alone for 24 h the actin and vinculin distribution and organization appears similar to the control. On the contrary using LY294002+ HGF or Src inhibitor-

1+ HGF the cytoskeleton remodelling observed after 24 h in the presence of the factor is reverted (Figure 26).



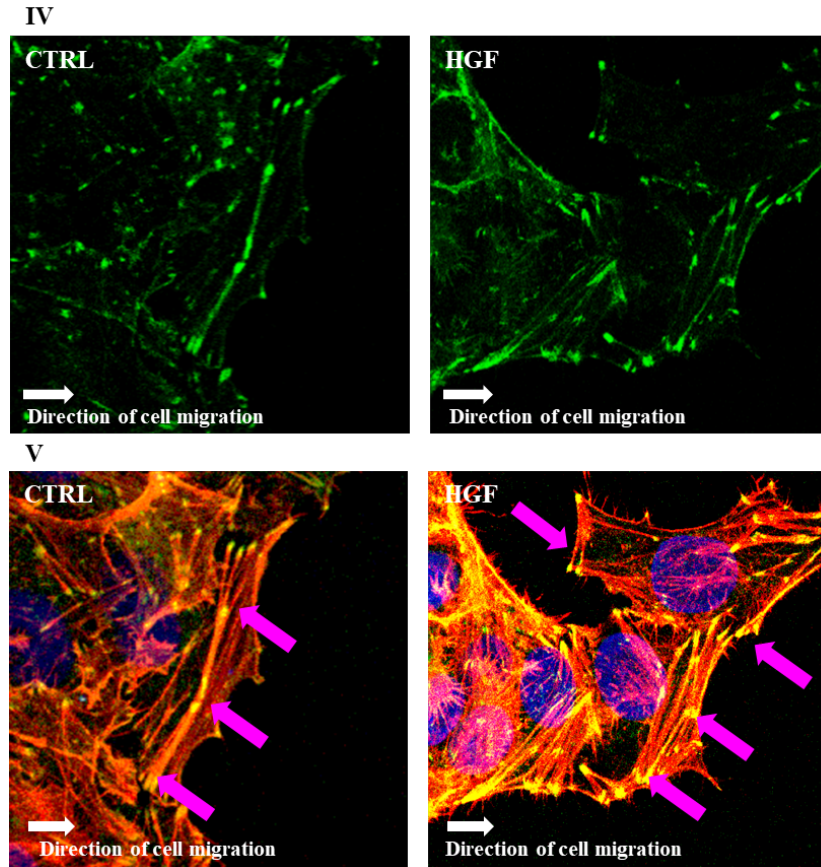


Figure 25: Representative images of Confocal Microscopy of F-actin (green) and Vinculin (green). I) Immunofluorescence of Vinculin in NT2D1 cells cultured with or without HGF, after 24h of the wound healing experiment. II) Actin cytoskeleton of control and HGF condition. III) Co-localization of vinculin and F-actin. Nuclei staining (blue signal) are also reported in the figure. IV) Electronic zoom of the vinculin in the control and HGF conditions. V) Electronic zoom of the colocalization of vinculin and actin. The presence of the vinculin in the leading edge in the HGF condition appears evident. In the panels I, II and III, scale bar is 35,7 μ M.

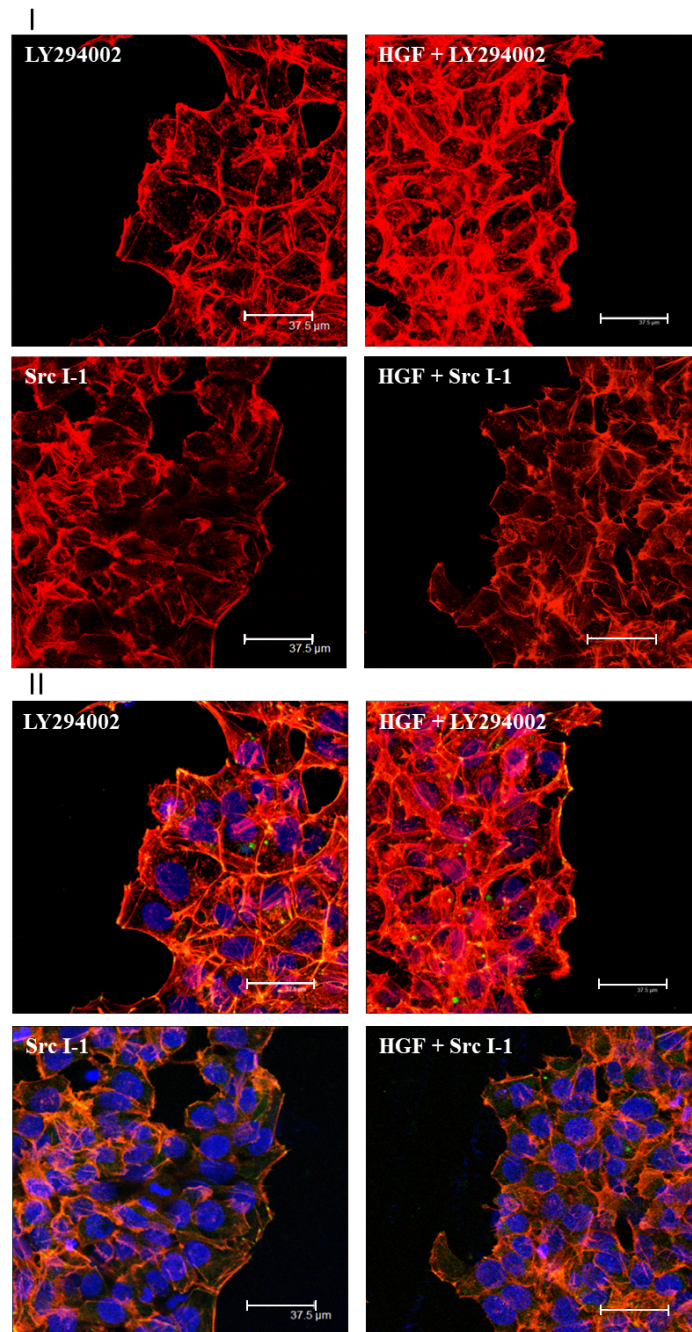


Figure 26: Representative images of confocal microscopy of F-actin (red) and Vinculin (green). I) Actin cytoskeleton of cells treated with Src inhibitor-1 and LY294002, either alone or with HGF. II) Co-localization of vinculin and F-actin. Nuclei staining (blue signal) are also reported in the figure. Scale bar 37,5 μ M.

4.5 HGF expression in TGCTs biopsies

4.5.1 HGF distribution pattern in TGCT histological samples

In our previous work, in collaboration with Prof. Looijenga of the Erasmus Medical Center of Rotterdam, we evaluated c-MET expression in histological samples derived from all type II TGCTs patients (102). In detail, we observed that GCNIS shows clear membranous staining of c-MET protein, and, in some cases, a nuclear staining. SE tumours demonstrated a lower membranous staining, a weak diffused cytoplasmic pattern and negative nuclei. Notably, EC histological type results in a higher membranous expression, a diffused cytoplasmic signal and nuclei totally negative. In general, c-MET positivity results very strong, especially in more differentiated (teratoma) and more aggressive TGCTs (yolk sac tumours and choriocarcinoma).

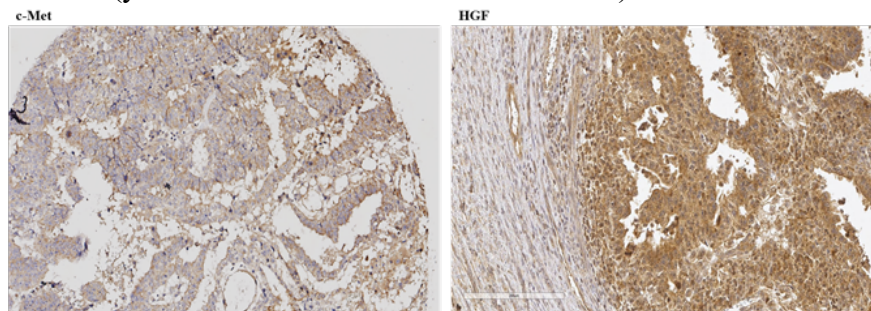


Figure 26: Representative images of ICH performed on EC slides. ICH assay using anti-c-MET and anti-HGF.

Since NT2D1 cells origin from EC lesion, herein, we report the HGF immunoreactivity in samples derived from patients affected by EC from different histological collections. In EC samples obtained by institute Pascale collection we observed that EC cells

express high levels of HGF, while, at the same time, these EC cells expressed c-MET in the cellular membrane (Figure 26). This finding suggests that HGF acts in patients in an autocrine way, whereas in vitro NT2D1 cells did not express and secrete HGF (102).

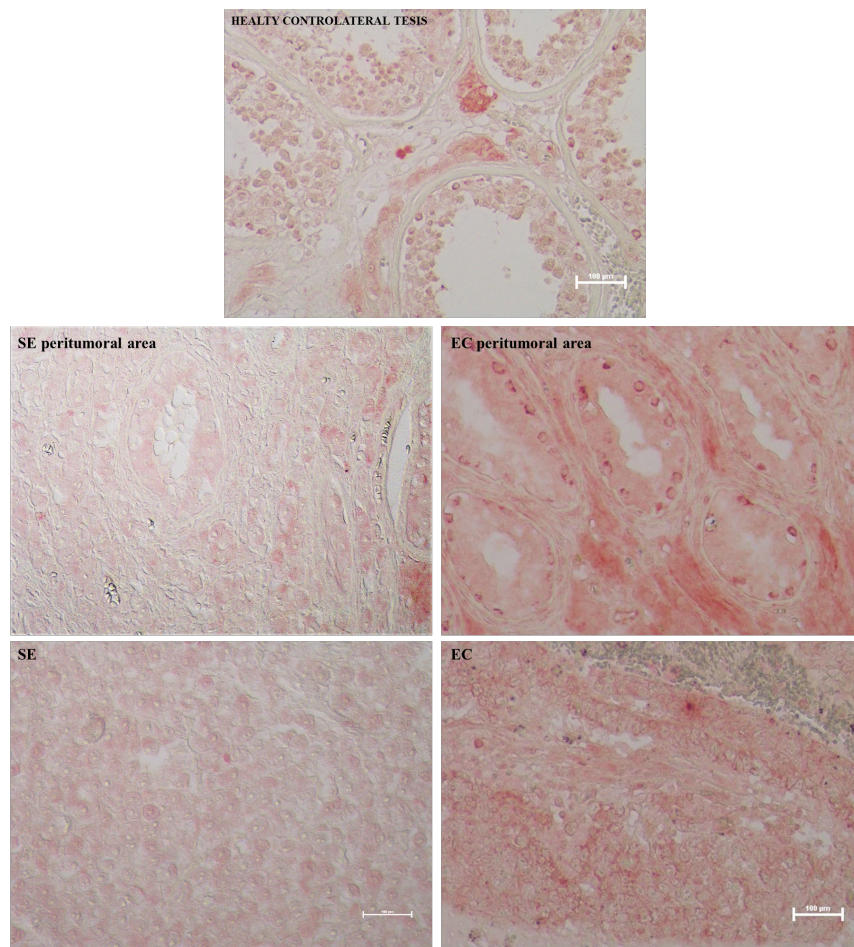


Figure 27: Representative images of HGF immunoreactivity in SE and EC and their peritumoral area samples. Representative image of healthy contralateral testis is also reported. Three different patients affected by SE tumours and one patients of EC are analysed.

Moreover, analysing the histological TGCT sample collection of Prof. Andrea Isidori of Sapienza University of Rome, we observed the HGF expression in SE and EC lesions (Figure 27). HGF appears mainly localized in the cytoplasm of SE cells, whereas it is more widely distributed in EC lesions. Overall, it is worth to highlight that EC cells show higher level of HGF expression than SE samples. Intriguingly, we observed that also EC peritumoral area demonstrates stronger immunoreactivity with respect to the SE counterpart (Figure 27). In particular, atrophic tubules of EC peritumoral areas show a featured perinuclear HGF signal in basal germ cells.

We analysed also the HGF expression in the healthy contralateral testis of TGCT affected patients and we observed that both seminiferous epithelium and Leydig cells clearly express this growth factor. This pattern of distribution overlaps with c-MET localization. It would be interesting to investigate if this autocrine fashion of HGF/c-MET system is acquired due to the altered microenvironment of the parenchima. To this aim, the analysis of c-MET and HGF distribution pattern should be performed on healthy donors (Figure 28).

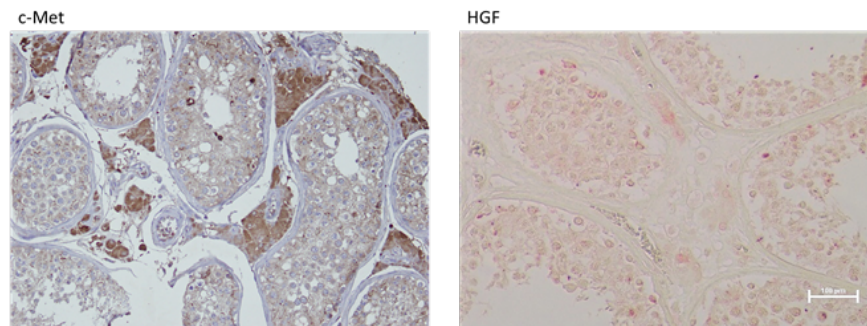


Figure 28: Healthy contralateral testis of TGCT affected patients.

Erica Leonetti

Discussion

As previously mentioned, all type II TGCTs origin from a common precursor lesion, called Germ Cell Neoplasia In Situ (GCNIS). This lesion can give rise to seminoma (SE) or embryonal carcinoma (EC) tumours, being EC in turn the precursor of all non-seminoma tumours (NST) (as well as choriocarcinoma, yolk salk tumours and teratoma). SE and NST appear very different: SE manifests undifferentiated gonocytes features, while NST appears more heterogeneous. Moreover, SE are characterized by blocked gonocytes, which express germ cell specific genes, whereas EC is a malignant caricature of embryonic stem cells due to a genomic reprogramming of GCNIS with up-regulation of pluripotency genes. The difference is also evident in the degree of tumour aggressiveness, which affects the prognosis of the disease: NST are generally more aggressive than SE ones and affect younger men (2). The main clinical interest about these cancers (that are mostly chemo- and radio- sensitive), is represented by: 1) a fraction of patients chemo- and radio- resistant, 2) the long-term morbidity associated with the use of the chemotherapeutics. Even if several Genome-Wide Association Studies (GWAS) revealed important loci variants in TGCTs (28, 91, 99, 100, 107, 108), very few targetable mutated genes have been discovered so far, in spite of the high aneuploidy that features these cancer types (109).

c-MET and its ligand HGF are expressed during embryogenesis and are also involved in the maintenance of tissue homeostasis and wound repair. Notably, *c-MET* is also a proto-oncogene, and it appears involved in the onset and progression of several solid tumours. *c-MET* is encoded on chromosome 7, 7q31 region (59). Noteworthy, it was demonstrated the gain of function of chromosome 7 in patients affected by TGCTs, and, very recently, it was also described that high serum levels of HGF correlates with a cancer progression (101). These observations allowed us to hypothesize that HGF/*c-MET* system as a role in TGCT physiology. In a previous work, in fact, we demonstrated that *c-MET* is expressed in three cell lines representative of different

histo-types of TGCTs. Interestingly, the non-seminoma cell line, called NT2D1, demonstrated the highest HGF-sensitivity when compared to TCam-2 (representative of seminoma tumours) and NCCIT (representative of mixed tumours) cell lines; in fact, NT2D1 cells modify their proliferating, migrating and invading attitude when stimulated with the growth factor (102).

Starting from this data, we decided to continue our analysis on NT2D1 to better understand the molecular mechanisms involved in these HGF-dependent responses. To this purpose, in the first part of this elaborate we demonstrate the specificity of HGF-dependant NT2D1 responses, using a c-MET inhibitor. Chemotaxis and collective migration result consistently decreased in presence of the inhibitor, demonstrating that all these HGF-activated responses are dependent on c-MET activation. These results are part of a recent published work (103).

It is well known that the HGF/c-MET system is a very intricate signalling, whose activation determines a complex pathway activation cascade (59). Among the numerous adaptor proteins activated by c-MET, c-Src and PI3K/AKT represent two of the most studied ones.

Herein, we demonstrate that c-Src is implicated in NT2D1 HGF-dependent responses. More in detail, using a pharmacological approach we observed that c-Src is involved in HGF-dependent cell proliferation, chemotaxis, collective migration, cytoskeleton reorganization and invasion in NT2D1 cells. In fact, cells treated with HGF, in combination with the inhibitor of c-Src, reverted to the control values, indicating the implication of c-Src in these cellular functions. Since Vinculin and Actin are two main characters of the cell motility, the study of their localization is useful to confirm the role of HGF to improve aggressive capability in NT2D1 cells. The co-localization of F-actin and Vinculin in HGF treated cells is observed especially at the leading edge of the cellular membrane indicating the formation of new focal adhesion structures, related to cell migration. The inhibition of c-Src results in a reversion of this phenomenon.

Notably, c-Src appears constitutively activated in these cell line. Western blot analysis reveals, in fact, that the active form of c-Src is detectable in these cells even when cultured in basal conditions, and, surprisingly, it is not significantly modulated by HGF administration. Nevertheless, immunofluorescence analyses revealed that HGF treatment determines the translocation of active c-Src into the nucleus, indicating a recruitment of this adaptor-protein in the direct modulation of cellular transcription downstream c-MET signalling pathway. Noteworthy, recent literature data reported the hypothesis according to which c-Src (phospho Tyr 416) may change its localization, and that the biological meaning related to this different distribution is cell-dependent (104-106). Surprisingly, treatments with Src inhibitor-1 alone increase NT2D1 invasiveness and, at the same time, decrease the cell-proliferation rate and collective migration capability of NT2D1 cells in an HGF-independent way. Based on these results, we can hypothesize that c-Src is recruited by c-MET when this receptor is activated by HGF, but that in absence of HGF it can also be recruited by other related pathways in NT2D1 cells. In this regard, it is fair to mention that it was recently demonstrated (42) a panel of tyrosine kinase receptors constitutively phosphorylated in NT2D1 cells. These observations suggest the important role involved by microenvironment in NT2D1 biological responses. Part of these results is reported in our recent work (103).

In this work we also proved that PI3K/AKT pathway appears involved in NT2D1 responses. Herein, we observed that HGF determines AKT phosphorylation, and its consequent activation. Through proliferation, chemotaxis, wound healing and invasion assays, we demonstrated that the HGF-related higher aggressive behaviour in NT2D1 cells is reverted when the inhibition of PI3K/AKT pathway occurs. In line with these results, morphological analysis shows the involvement of this pathway in HGF-dependent aggressive capabilities in NT2D1 cells. In fact, HGF samples analyzed by electronic microscopy reveals strong reactivity of cell membrane, with microvesicles formation on the

cell surface and numerous membrane protrusions. The use of the inhibitor, in combination with HGF, determines absence of membrane reactivity, similar to the control condition. This analysis suggests the role of PI3K/AKT pathway in NT2D1 HGF-dependent aggressive behaviour.

Interestingly, similar to c-Src inhibitor, the use of LY294002 alone causes higher aggressive behavior of NT2D1 cells in invasion, actin/vinculin co-localization and membrane activity. However, it causes a reduction of their collective migration. Therefore, we can hypothesize that, also in this case, the microenvironment plays an essential role and that the absence or the presence of several growth factors, as well as HGF, determine different biological responses. PI3K/AKT can be recruited by c-MET in an HGF-dependent way, and also by housekeeping homeostatic pathways that balance the aggressive behaviour of NT2D1 cells.

Based on these results, it appears clear that both pathways exert a similar function in NT2D1 cells. Since literature data show a strong correlation between c-Src and PI3K/AKT pathways, herein we show preliminary results on the possible link between these two signalling cascades in NT2D1 cells. The use of the Src inhibitor-1 determined a reduction of AKT phosphorylation, suggesting the possible correlation between these two signalling. Obviously, further investigation is needed to better clarify this hypothesis.

As a further analysis, immunoreactivity of HGF on slides derived from EC patients is localized on the cellular membrane of the same cells where c-MET expression in other patients was previously (102) demonstrated, suggesting the HGF autocrine secretion in these cancer lesions. Noteworthy, EC slides show higher level of HGF expression with respect to SE samples. The presence of high levels of HGF in these cancer lesions suggests an involvement of the HGF/c-MET system in the onset of more aggressive forms of type II TGCTs.

Highlights

Even if type II TGCTs have, in most cases, a good prognosis, a little percentage of patients develops drug resistance or long-term toxicity. For this reason, a better knowledge of the pathophysiology of these lesions is required. To this aim, we studied TGCT responses to RTKs, demonstrating the following:

- c-MET is expressed in type II TGCTs and HGF is active predominantly on non-seminoma derived cells, such as NT2D1 cells, triggering their proliferation, migration and invasion.
- Analysing two c-MET-activated pathways (c-Src and PI3K/AKT), which are known to be involved in the onset and progression of several human cancers, we observed that their inhibition reversed the HGF-dependent cellular responses.
- Noteworthy, the effect of c-Src and PI3K inhibitors in HGF-free culture system revealed, in some cases, paradoxical effects, improving NT2D1 cells aggressiveness. This observation highlights the importance of the microenvironment in the modulation of NT2D1 cell aggressiveness.

In light of these observations, we can speculate that the presence of HGF, as well as of its amount, in the testicular microenvironment could determine a different response to possible therapies that target c-MET signaling pathway. In this regard, we started to analyse, by immunohistochemistry, the amount of HGF in biopsies derived from patients affected by type II TGCTs, and we observed that Embryonal Carcinoma show a higher level of HGF with respect to Seminoma tumours. Deeper investigations are needed to clarify the mechanisms involved in this process, but the results herein reported appear very promising in the study of TGCTs cancer progression and open new horizons in the development of more personalized target therapies.

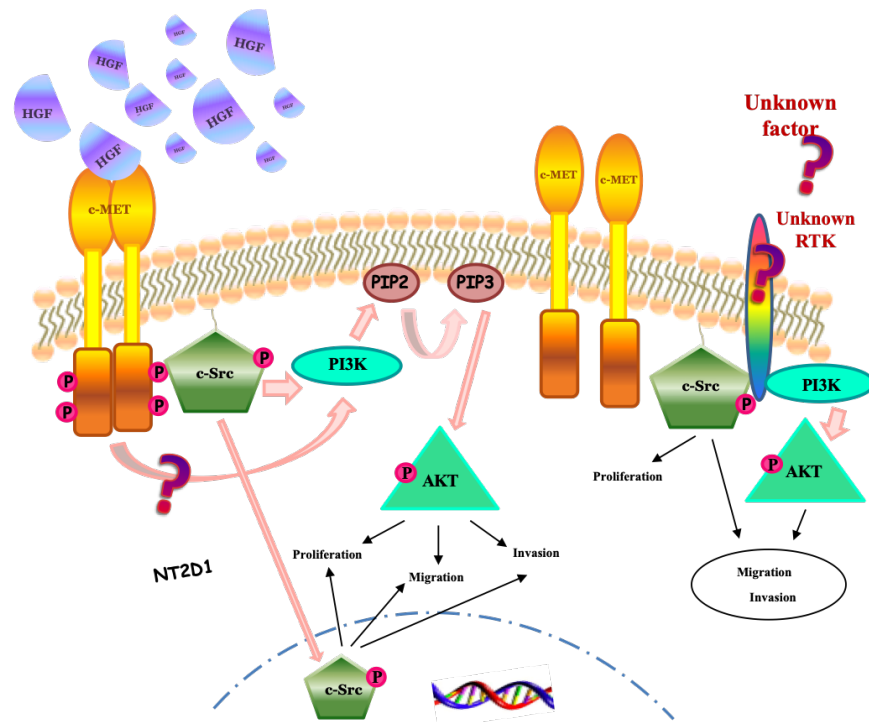


Figure 29: Graphical Abstract: Proposed model of our system in the light of the presented data. HGF administration in NT2D1 cells determines activation of c-MET. It activates c-Src protein, which, in turn, can recruit PI3K. Alternatively PI3K can be directly activated by c-MET phosphorylation. As a consequence of PI3K activation, AKT results phosphorylated and is responsible for NT2D1 biological responses, such as proliferation, migration and invasion. Even c-Src recruitment and its translocation in the nucleus seem to be involved in NT2D1 cell malignant behaviour (proliferation, migration and invasion). Moreover, it is worth to highlight that some RTKs are known to be constitutively activated in NT2D1 cells. Therefore, unknown factors can activate unknown RTKs triggering c-Src and/or PI3K/AKT signalling in HGF-independent manner.

5. Materials and Methods

5.1 Cell Culture

NT2D1 embryonal carcinoma cells were purchased from the ATCC. This cell line was cultured in DMEM (Sigma Aldrich, cat. D6546, St Louis, MO, USA) supplemented with 10% Foetal Bovine Serum (FBS Gibco, cat. 10270, Gland Island, NY, USA), L-Glutamine (Sigma Aldrich, cat. G7513) and penicillin/streptomycin (Sigma-Aldrich, cat. P0781). The cells were used from passage 15 to 35. Mycoplasma testing was routinely done with the N-GARDE Mycoplasma PCR Reagent set (Euro-Clone, cat. EMK090020, Milano, Italy). The cells were treated with 40 ng/mL of HGF (Human Recombinant HGF, R&D Systems, cat. 294-HG, Minneapolis, MN, USA), 50 μ M of a c-MET specific inhibitor (PF04217903; Sigma-Aldrich, cat. SML0263), 5 μ M of a Src inhibitor (Src Inhibitor-1; Sigma-Aldrich, cat. S2075), or 5 μ M of a PI3K inhibitor (LY294002; Cayman chemical, cat. 70920). We tested different concentrations of c-Src inhibitor and PI3K inhibitor (1 μ M to 10 μ M and 1 μ M to 15 μ M, respectively) on cell viability. 5 μ M, was the highest concentration without toxic effect evaluated by trypan blue exclusion test for both inhibitors, while PF04217903 was used as already described in a recent work (102).

5.2 Cell Proliferation Assay

Proliferation assays was performed using or c-MET inhibitor, or c-Src inhibitor-1 or LY294002. We cultured 9×10^4 NT2D1 cells in 12-well plates in DMEM 10% FBS. After 24 h, the cells were starved for 16 h under serum-free conditions, and then were treated with DMEM 2% FBS (control condition), adding, when indicated, HGF alone, Src inhibitor-1, LY294002, LY294002 + HGF or Src inhibitor-1 + HGF. After 48h, cells were trypsinized, harvested, and counted. Each experiment was performed at least in triplicate. Four independent experiments were performed. The results (Mean

± SEM) are expressed as fold-change considering control condition as 1.

5.3 Cell Cycle FACS Analysis

Cells were seeded at 5×10^5 cells in 60 mm petri dishes. After 24 h cells were maintained under serum-free conditions for 16 h (starvation). Then, cells were cultured for different times (6, 24, 30 and 48 h) in the absence or in the presence of Src inhibitor-1 (5 μ M) in 2% FBS. The cells were harvested, fixed in 70% Et-OH at 4 °C, and stained with propidium iodide (50 μ g/mL)/RNase (100 U/mL) solution (Sigma-Aldrich, cat. P4864 and R6513 respectively) for at least 3 h. The cell suspensions were analysed with CyAn ADP (Beckman Coulter, Fullerton, CA, USA) and data were analyzed with the FCS Express 5.1 software (De Novo, Los Angeles, CA, USA).

5.4. Cell Death Assay

Cells, maintained under serum-free conditions for 16 h, were treated with Src inhibitor-1 or LY294002 at different concentrations (1, 2.5, 5 and 10 μ M for Src inhibitor-1 while 1, 5, 10 and 15 μ M for LY294002) for 48 h. Src inhibitor-1 was also tested alone at 5 μ M for 72 h. Since Src inhibitors and LY294002 were soluble in Dimethyl Sulfoxide (DMSO), the respective dose of DMSO alone was added to control samples. Cell death was evaluated with propidium iodide exclusion assay, using 2 μ g/mL of propidium iodide (Sigma- Aldrich, cat. P4864). Cell death was evaluated by flow cytometry using CyAn ADP (Beckman Coulter), and data were analyzed with the FCS Express 5.1 software (De Novo).

5.5 Chemotaxis Assay

Chemotaxis assay was performed using the Cell Culture Inserts (12 well 8.0 μ m pore size; Falcon, cat. 353182, Lincoln Park, NJ, USA) placed in 12-well culture plates (Falcon, cat. 351143). Cells were starved for 16 h under serum free conditions. Part of the cells were

pre-treated with DMEM 10% FBS+PF-04217903 for 30 min, to inhibit c-MET phosphorylation, with DMEM 10% FBS + Src inhibitor-1 for 48 h, to inhibit c-Src phosphorylation, or with LY294002 for 1 h to inhibit PI3K. Then, cells were trypsinized, counted, and re-suspended in DMEM without serum. 2×10^5 cells/well in 1.4 mL DMEM were added in the upper chamber of the trans-well, in absence (DMEM alone), or in presence of PF-04217903, Src inhibitor-1 or LY294002. The lower chambers were filled with 800 μ L DMEM alone (negative control) or DMEM+HGF. Cells were incubated at 37 °C with 5% CO₂. After 5 h, the medium and un-migrated cells, in the upper surface of the insert, were mechanically removed, and the lower surface of the insert, containing migrated cells, was fixed with paraformaldehyde 4% in PBS (pH 7.4) at 4 °C, and stained with Diff Quick solution (DADE, cat. 130832, Network, NJ, USA). Migrated cells were visualized under 40x objective using a bright-field Optical Microscopy (Axioplan, Zeiss, Oberkochen, Germany). For cell counting, each filter was divided in sectors and all sectors of each filter were photographed under the 40x magnification objective and counted. In this way, we considered to have approximately counted the whole area of each filter. The migrated cells were counted manually, with the help of ImageJ software. Three independent experiments were performed. Each experiment was performed at least in quadruplicate. The results (Mean \pm SEM) are expressed as fold-change being control condition arbitrarily considered as 1.

5.6 Wound-healing Assay (Collective Migration Assay)

To perform the wound-healing assay, we used special double well culture inserts (Ibidi GmbH, Martinsried, Germany). Each insert was placed in a well of a 24-well plate. Cells were starved for 16 h under serum free conditions, then they were detached, and 3.5×10^4 cells were placed into both wells of each insert with 70 μ L of medium containing 2% FBS. When cells are confluent, the culture inserts were gently removed, and cells were fed with 2% FBS

DMEM (CTRL), or treated with HGF (40 ng/mL), PF-04217903 (50 μ M), HGF+PF-04217903, Src inhibitor-1 (5 μ M), HGF+ Src inhibitor-1, LY294002 (5 μ M), HGF+ LY294002 all diluted in CTRL medium. Each well was photographed at 10x magnification immediately after insert removal, for the measurement of the wound (cell-free) area (T0 area considered as 100%), and after 24 h and 48 h with a Nikon DS-Fi1 camera (Nikon Corporation, Tokyo, Japan), coupled with a Zeiss Axiovert optical microscope (Zeiss, Oberkochen, Germany). The mean percentage of residual open area compared with the respective cell-free space taken at T0 was calculated using ImageJ v 1.47 h software. For each experimental condition, four independent experiments were performed in triplicate.

5.7 Matrigel Invasion Assay

For assessment of invasion, in vitro invasion assay was performed using chambers coated with GFR-Matrigel (Basement Membrane Matrix Growth Factor Reduced, BD Biosciences, cat. 354483, San Jose, CA, USA). Cells were starved for 16 h in DMEM without FBS and then were pre-treated with Src inhibitor-1 for 48 h or with LY294002 for 1 h. Cells were then trypsinized, counted and re-suspended. 2.5×10^4 cells/well in 500 μ L DMEM 2% FBS were seeded on the top of the GFR-Matrigel (control condition). When indicated, Src inhibitor-1, HGF, or Src inhibitor-1+HGF were added to cell suspension. The lower chambers were filled with 750 μ L DMEM supplemented with 2% FBS. Cells were incubated for 24 h at 37 °C with 5% CO₂, and then GFR-Matrigel and non-invading cells were mechanically removed with cotton swabs. Filters containing invading cells were fixed with paraformaldehyde 4% in PBS (pH 7.4) at 4°C and stained with Diff Quick solution. The filters were analysed by bright field Optical Microscopy and four fields per filter were photographed at 10x magnification to obtain a global view of cell invasion. For cell counting, each matrigel-coated filter was divided in sectors and all sectors of each filter were photographed under the 40X magnification objective

and counted. In this way, we considered to have approximately counted the whole area of each filter. The migrated cells were counted manually, with the help of ImageJ software. Invading cells were counted and the average number \pm SEM of cells are reported as fold change being control considered as 1. Three independent experiments were performed, and each experiment was performed at least in triplicate.

5.8 Immunofluorescence Analyses and actin staining

Different immunofluorescence experiments were performed in order to:

- Study the NT2D1 proliferation index after wound healing experiment with pHH3⁺ antibody;
- Observe the distribution pattern of the active form of c-Src;
- Observe the apoptosis rate using Cleaved Caspase-3 antibody;
- Describe the cytoskeleton changes analysing vinculin and actin.

Briefly, cells were fixed in paraformaldehyde 4% in PBS (pH 7.4) at 4 °C for 15 min, and permeabilized in PBS supplemented with 1% BSA and 0.1% Triton for 2 h. Then, samples were incubated overnight with the specific primary antibody: rabbit anti-c-Src (phospho Tyr 416) antibody (GeneTex n. GTX 81151; 1:25 dilution), rabbit anti-cleaved Caspase-3 antibody (Cell Signaling D175; 1:80 dilution), mouse anti-phospho-histone H3 antibody (pHH3 mouse monoclonal, Santa Cruz, cat. sc-374669, CA, USA, 1:50 dilution), mouse anti-vinculin (Santa Cruz, cat. sc-73614; 1:50 dilution). Then, samples were washed three times in PBS/BSA/Triton for 30 minutes and incubated with the appropriate secondary antibody: FITC-conjugated donkey anti-rabbit IgG (Jackson Immuno Research, cat. 711-095-152, West Grove, PA, USA, dil. 1:200), and FITC-conjugated donkey anti-mouse IgG (Jackson Immuno Research, cat. 715-095-150, dil. 1:200). TO-PRO3 iodide fluorescent dye 642/661 (1:5000 in PBS, Invitrogen, cat. T3605, Carlsbad, CA, USA) for nuclei staining and rhodamine

phalloidin (Invitrogen Molecular Probes Eugene 1:40 dilution) for F-actin visualization were used. Immunofluorescence experiments were analyzed using Leica Confocal Microscope (Laser Scanning TCS SP2 equipped with Kr/Ar and He/Ne lasers, Mannheim, Germany). Quantitative analysis, (Sum of Intensity (SUM (I)) of Phospho-Histone H3 positive cells and nuclei was performed by Leica Confocal software.

5.9 Western Blot Analyses

To better investigate the activation status of c-Src, the cells were cultured for 8, 12 and 18 h in DMEM 2% FBS with or without HGF. On the other hand, to investigate PI3K/AKT pathway, cells were cultured for 30' with HGF and the pathway inhibition was investigated treating cells with LY294002 for 1h. At the end of these culture times, cells were solubilized in lysis buffer (1% SDS, 10 mM Tris, pH 7.5) containing protease and phosphatase inhibitors (Roche, cat. 04693124001 and 04906837001, Mannheim, Germany). Protein concentration was determined using the BCA protein assay (Pierce, cat. 23221), and 40 µg/lane were loaded into 7% SDS-PAGE under reduction condition. Precision Plus Protein All Blue Standards (Bio-Rad Laboratories, Hercules, CA, USA) were used as molecular weight markers. Proteins were electro-transferred to nitrocellulose membranes (Bio-Rad, cat. 1620115). Membranes were blocked through incubation with 5% BSA (Sigma-Aldrich, cat. A2153) in TBS-T buffer (20 mM Tris, pH 7.6, 150 mM NaCl, 0.1% Tween-20), to avoid non-specific binding of the antibodies. Then, the membranes were incubated with anti-c-Src (all isoforms) antibody, raised in rabbit (Cell Signaling, cat. 2108, 1:1000 dilution), or anti-c-Src (phospho Tyr 416) antibody (GeneTex, GTX 81151; San Antonio, TX, USA, 1:100 dilution), or anti-c-Src (phospho Tyr 527) antibody (GeneTex, GTX 50210; 1:500 dilution), or anti-AKT (all isoforms) antibody (Cell Signaling, cat. 9272, 1:1000 dilution) or anti-p-AKT (S473) antibody (Cell Signaling cat. 4060, 1:1000 dilution). Primary antibodies were incubated for 16 h at 4 °C. For the

detection, nitrocellulose membranes were incubated with HRP conjugated secondary antibody Anti-Rabbit IgG (1:5000, GE Healthcare UK Limited, Buckinghamshire, England, cat. NA9340V). To normalize total protein extracts, monoclonal anti- α -actin directly conjugated with HRP (1:10.000, Sigma-Aldrich, cat. A3854) was used. For the band visualization, the ECL western blotting detection reagent, (Euroclone, cat. EMP011005) was used. Membranes were analysed by ChemiDoc XRS and the image acquired were processed by Image Lab software (Bio-Rad Laboratories). Phospho c-Src densitometric profiles have been normalized versus total c-Src/ α -actin as well as pAKT normalized versus total AKT/pAKT. Three independent experiments were performed, and each experiment was performed at least in duplicate.

5.10 Scanning Electron Microscopy

9×10^4 NT2D1 were cultured and treated with HGF and LY294002 for 24h. After that, samples were fixed in Glutaraldehyde 2.5% in cacodylate buffer 0.1 M pH 7.3 O.N. and then they were post-fixed with 1% osmium tetroxide in cacodylate buffer 1 M, dehydrated with increasing ethanol percentage (30–90% in water for 5 min, twice 100% for 15 min), treated in Critical Point Dryer (EMITECH K850), sputter coated with platinum-palladium (Denton Vacuum DESKV), and observed with Supra 40 FESEM (Zeiss).

5.11 Immunohistochemical Analyses

Slides were prepared from biopsies of patients affected by Type II TGCTs embedded in paraffin. Sections were dewaxed with toluene, hydrated with decreasing scale of alcohols, and rinsed with dH₂O and PBS without Ca⁺⁺ and Mg⁺⁺. Endogenous peroxidases were blocked using Hydrogen Peroxide Block (KIT Abcam, cat. ab236467) for 10 minutes at room temperature. After two washes in PBS1x, sections were subjected to antigen retrieval procedure with Tris-EDTA buffer (10 mM Tris base, 1 mM EDTA

solution, 0.05% Tween 20, pH 9.0): for 10 minutes at high temperature. To avoid possible background, samples were treated with Protein Block (KIT Abcam, cat. ab236467) for 30 minutes. Primary antibody anti-HGF (Abcam, cat. ab83760, 1:60 dilution) was incubated over night at 4°C. After washes, Goat anti-rabbit HRP Conjugate was used for 1 h at room temperature. Then, three washes with PBS1x were realized and at the end AEC Single solution (KIT Abcam, cat. ab236467) or 3, 3'-diaminobenzidine (Dako, cod. K3468) was used. Nuclei were stained with ematosilin solution. Samples were analyzed by optical microscopy Nikon Eclipse. Negative controls were processed in the absence of the primary antibody and pre-immune isotype rabbit immunoglobulins (1:1000 dilution).

5.12 Statistical Analyses

All quantitative data are presented as the mean \pm standard error (SEM). The statistical analyses have been carried-out using Sigma Plot 11 Data Analyzer Software. Student's t-test and ANOVA test (for multi-group comparison) were carried-out. Data-Analyzer Software chose the ANOVA's post-hoc tests, depending on data distribution. In detail, Fisher's Least Significant Difference (LSD) was applied to all the ANOVA tested experimental data, except for wound-healing data that were analysed.

6. List of abbreviations

BSA: Bovine Serum Albumine
CBL: Casitas B-lineage Lymphoma
CHC: Choriocarcinoma
c-MET: Mesenchymal Epithelial Transition
DSD: Disorders of sex development
EC: Embryonal Carcinoma
EGFR: Epidermal Growth Factor
FAK: Focal Adhesion Kinases
FBS: Foetal Bovine Serum
GAB: GRB2 associated binding protein
GCNIS: Germ Cell Neoplasia In Situ
GCT: Germ Cell Tumour
GRB2: growth factor receptor bound protein 2
HGF: Hepatocyte Growth Factor
HGFA: HGF activator
IPT: immunoglobulin plexins transcription
HAI: HGF Activator Inhibitor
MAPK: mitogen activated kinase-like protein
mTOR: mammalian target of rapamycin
NSCLC: Non-Small Cell Lung Cancer
NST: non-seminoma tumour
PLC: phospholipase C
PGC: Primordial Germ Cell
PI3K: phosphoinositide-3-kinase
PIP2: Phosphatidylinositol (4,5)-bisphosphate
PIP3: phosphatidylinositol (3,4,5)-trisphosphate
PSI: Plexin, Semaphorin and Integrin cysteine-rich
RTK: Receptor Tyrosine Kinase
S.E.M.: Standard Error Measure
SE: Seminoma
SEM: Scanning Electron Microscopy
SHC: Src homology 2 domain containing
SKI-1: src inhibitor- 1 or Src I-
STAT: signal transducer and activator of transcription

Erica Leonetti

TDS: Testicular Dysgenesis Syndrome

TE: teratoma

TGCT: Testicular Germ Cell Tumour

TGF- α : Transforming Growth Factor

tPA: tissue Plasminogen Activator

uPA: urokinase Plasminogen Activator

VEGFR: Vascular Endothelial Growth Factor

YST: Yolk Sac Tumour

7. References

1. Friedman NB, Moore RA: Tumors of the testis; a report on 922 cases. *J Urol.* 1947, *57*:1199-1201.
2. Lobo J, Gillis AJM, Jeronimo C, Henrique R, Looijenga LHJ: Human Germ Cell Tumors are Developmental Cancers: Impact of Epigenetics on Pathobiology and Clinic. *Int J Mol Sci.* 2019, *20*.
3. Stang A, Trabert B, Wentzensen N, et al.: Gonadal and extragonadal germ cell tumours in the United States, 1973-2007. *Int J Androl.* 2012, *35*:616-625.
4. Chia VM, Quraishi SM, Devesa SS, et al.: International trends in the incidence of testicular cancer, 1973-2002. *Cancer Epidemiol Biomarkers Prev.* 2010, *19*:1151-1159.
5. Oosterhuis JW, Kersemaekers AM, Jacobsen GK, et al.: Morphology of testicular parenchyma adjacent to germ cell tumours. An interim report. *APMIS.* 2003, *111*:32-40; discussion 41-32.
6. Spoor JA, Oosterhuis JW, Hersmus R, et al.: Histological Assessment of Gonads in DSD: Relevance for Clinical Management. *Sex Dev.* 2018, *12*:106-122.
7. Kristensen DM, Sonne SB, Ottesen AM, et al.: Origin of pluripotent germ cell tumours: the role of microenvironment during embryonic development. *Mol Cell Endocrinol.* 2008, *288*:111-118.
8. Rajpert-De Meyts E, Skakkebaek NE, Toppari J: Testicular Cancer Pathogenesis, Diagnosis and Endocrine Aspects. In K. R. Feingold, B. Anawalt, A. Boyce, et al. (eds), *Endotext.* South Dartmouth (MA), 2000.
9. Skakkebaek NE: Possible carcinoma-in-situ of the testis. *Lancet.* 1972, *2*:516-517.
10. Berney DM, Looijenga LH, Idrees M, et al.: Germ cell neoplasia in situ (GCNIS): evolution of the current nomenclature for testicular pre-invasive germ cell malignancy. *Histopathology.* 2016, *69*:7-10.

11. Znaor A, Lortet-Tieulent J, Jemal A, Bray F: International variations and trends in testicular cancer incidence and mortality. *Eur Urol.* 2014, *65*:1095-1106.
12. Rosen A, Jayram G, Drazer M, Eggener SE: Global trends in testicular cancer incidence and mortality. *Eur Urol.* 2011, *60*:374-379.
13. Shanmugalingam T, Soultati A, Chowdhury S, Rudman S, Van Hemelrijck M: Global incidence and outcome of testicular cancer. *Clin Epidemiol.* 2013, *5*:417-427.
14. Trabert B, Chen J, Devesa SS, Bray F, McGlynn KA: International patterns and trends in testicular cancer incidence, overall and by histologic subtype, 1973-2007. *Andrology.* 2015, *3*:4-12.
15. Jorgensen A, Lindhardt Johansen M, Juul A, et al.: Pathogenesis of germ cell neoplasia in testicular dysgenesis and disorders of sex development. *Semin Cell Dev Biol.* 2015, *45*:124-137.
16. Skakkebaek NE, Rajpert-De Meyts E, Main KM: Testicular dysgenesis syndrome: an increasingly common developmental disorder with environmental aspects. *Hum Reprod.* 2001, *16*:972-978.
17. Hemminki K, Li X: Familial risk in testicular cancer as a clue to a heritable and environmental aetiology. *Br J Cancer.* 2004, *90*:1765-1770.
18. Rajpert-De Meyts E, McGlynn KA, Okamoto K, Jewett MA, Bokemeyer C: Testicular germ cell tumours. *Lancet.* 2016, *387*:1762-1774.
19. Ferlin A, Ganz F, Pengo M, et al.: Association of testicular germ cell tumor with polymorphisms in estrogen receptor and steroid metabolism genes. *Endocr Relat Cancer.* 2010, *17*:17-25.
20. Kristiansen W, Andreassen KE, Karlsson R, et al.: Gene variations in sex hormone pathways and the risk of testicular germ cell tumour: a case-parent triad study in a Norwegian-Swedish population. *Hum Reprod.* 2012, *27*:1525-1535.

21. Cook MB, Akre O, Forman D, et al.: A systematic review and meta-analysis of perinatal variables in relation to the risk of testicular cancer--experiences of the son. *Int J Epidemiol.* 2010, *39*:1605-1618.
22. Cook MB, Trabert B, McGlynn KA: Organochlorine compounds and testicular dysgenesis syndrome: human data. *Int J Androl.* 2011, *34*:e68-84; discussion e84-65.
23. McGlynn KA, Trabert B: Adolescent and adult risk factors for testicular cancer. *Nat Rev Urol.* 2012, *9*:339-349.
24. Daling JR, Doody DR, Sun X, et al.: Association of marijuana use and the incidence of testicular germ cell tumors. *Cancer.* 2009, *115*:1215-1223.
25. Trabert B, Sigurdson AJ, Sweeney AM, Strom SS, McGlynn KA: Marijuana use and testicular germ cell tumors. *Cancer.* 2011, *117*:848-853.
26. Geurts van Kessel A, van Drunen E, de Jong B, et al.: Chromosome 12q heterozygosity is retained in i(12p)-positive testicular germ cell tumor cells. *Cancer Genet Cytogenet.* 1989, *40*:129-134.
27. Oosterhuis JW, Castedo SM, de Jong B, et al.: A malignant mixed gonadal stromal tumor of the testis with heterologous components and i(12p) in one of its metastases. *Cancer Genet Cytogenet.* 1989, *41*:105-114.
28. Mostert MC, Verkerk AJ, van de Pol M, et al.: Identification of the critical region of 12p over-representation in testicular germ cell tumors of adolescents and adults. *Oncogene.* 1998, *16*:2617-2627.
29. Korkola JE, Houldsworth J, Bosl GJ, Chaganti RS: Molecular events in germ cell tumours: linking chromosome-12 gain, acquisition of pluripotency and response to cisplatin. *BJU Int.* 2009, *104*:1334-1338.
30. Looijenga LH, Rosenberg C, van Gurp RJ, et al.: Comparative genomic hybridization of microdissected samples from different stages in the development of a seminoma and a non-seminoma. *J Pathol.* 2000, *191*:187-192.

31. Ottesen AM, Skakkebaek NE, Lundsteen C, et al.: High-resolution comparative genomic hybridization detects extra chromosome arm 12p material in most cases of carcinoma in situ adjacent to overt germ cell tumors, but not before the invasive tumor development. *Genes Chromosomes Cancer*. 2003, 38:117-125.
32. Ottesen AM, Larsen J, Gerdes T, et al.: Cytogenetic investigation of testicular carcinoma in situ and early seminoma by high-resolution comparative genomic hybridization analysis of subpopulations flow sorted according to DNA content. *Cancer Genet Cytogenet*. 2004, 149:89-97.
33. Kraggerud SM, Skotheim RI, Szymanska J, et al.: Genome profiles of familial/bilateral and sporadic testicular germ cell tumors. *Genes Chromosomes Cancer*. 2002, 34:168-174.
34. Skotheim RI, Monni O, Mousses S, et al.: New insights into testicular germ cell tumorigenesis from gene expression profiling. *Cancer Res*. 2002, 62:2359-2364.
35. Looijenga LH, de Leeuw H, van Oorschot M, et al.: Stem cell factor receptor (c-KIT) codon 816 mutations predict development of bilateral testicular germ-cell tumors. *Cancer Res*. 2003, 63:7674-7678.
36. McIntyre A, Gilbert D, Goddard N, Looijenga L, Shipley J: Genes, chromosomes and the development of testicular germ cell tumors of adolescents and adults. *Genes Chromosomes Cancer*. 2008, 47:547-557.
37. Goddard NC, McIntyre A, Summersgill B, et al.: KIT and RAS signalling pathways in testicular germ cell tumours: new data and a review of the literature. *Int J Androl*. 2007, 30:337-348; discussion 349.
38. Pathak A, Stewart DR, Faucz FR, et al.: Rare inactivating PDE11A variants associated with testicular germ cell tumors. *Endocr Relat Cancer*. 2015, 22:909-917.
39. Oram SW, Liu XX, Lee TL, Chan WY, Lau YF: TSPY potentiates cell proliferation and tumorigenesis by promoting cell

cycle progression in HeLa and NIH3T3 cells. *BMC Cancer*. 2006, 6:154.

40. Looijenga LH, Gillis AJ, Oosterhuis JW: A pure triphasic testicular wilms tumor of primordial germ cell origin. *Urology*. 2008, 72:232-233; author reply 233.

41. Nathanson KL, Kanetsky PA, Hawes R, et al.: The Y deletion gr/gr and susceptibility to testicular germ cell tumor. *Am J Hum Genet*. 2005, 77:1034-1043.

42. Selfe J, Goddard NC, McIntyre A, et al.: IGF1R signalling in testicular germ cell tumour cells impacts on cell survival and acquired cisplatin resistance. *J Pathol*. 2018, 244:242-253.

43. Das MK, Kleppa L, Haugen TB: Functions of genes related to testicular germ cell tumour development. *Andrology*. 2019, 7:527-535.

44. Killian JK, Dorssers LC, Trabert B, et al.: Imprints and DPPA3 are bypassed during pluripotency- and differentiation-coupled methylation reprogramming in testicular germ cell tumors. *Genome Res*. 2016, 26:1490-1504.

45. Rijlaarsdam MA, Tax DM, Gillis AJ, et al.: Genome wide DNA methylation profiles provide clues to the origin and pathogenesis of germ cell tumors. *PLoS One*. 2015, 10:e0122146.

46. Costa AL, Lobo J, Jeronimo C, Henrique R: The epigenetics of testicular germ cell tumors: looking for novel disease biomarkers. *Epigenomics*. 2017, 9:155-169.

47. Chieffi P: An Overview on Predictive Biomarkers of Testicular Germ Cell Tumors. *J Cell Physiol*. 2017, 232:276-280.

48. Maroto P, Anguera G, Martin C: Long-term toxicity of the treatment for germ cell-cancer. A review. *Crit Rev Oncol Hematol*. 2018, 121:62-67.

49. Chovanec M, Abu Zaid M, Hanna N, et al.: Long-term toxicity of cisplatin in germ-cell tumor survivors. *Ann Oncol*. 2017, 28:2670-2679.

50. Gerl A, Sauer H, Liedl B, Hiddemann W: [The therapy of testicular tumors 2 decades after the introduction of cisplatin]. *Dtsch Med Wochenschr*. 2000, 125:327-334.

51. Schmidtova S, Kalavska K, Kucerova L: Molecular Mechanisms of Cisplatin Chemoresistance and Its Circumventing in Testicular Germ Cell Tumors. *Curr Oncol Rep.* 2018, 20:88.
52. Mizuno Y, Gotoh A, Kamidono S, Kitazawa S: [Establishment and characterization of a new human testicular germ cell tumor cell line (TCam-2)]. *Nihon Hinyokika Gakkai Zasshi.* 1993, 84:1211-1218.
53. de Jong J, Stoop H, Gillis AJ, et al.: Further characterization of the first seminoma cell line TCam-2. *Genes Chromosomes Cancer.* 2008, 47:185-196.
54. Nakamura T: [Molecular characterization of hepatocyte growth factor (HGF)]. *Seikagaku.* 1989, 61:1243-1247.
55. Seki T, Hagiya M, Shimonishi M, Nakamura T, Shimizu S: Organization of the human hepatocyte growth factor-encoding gene. *Gene.* 1991, 102:213-219.
56. Nakamura T, Mizuno S: The discovery of hepatocyte growth factor (HGF) and its significance for cell biology, life sciences and clinical medicine. *Proc Jpn Acad Ser B Phys Biol Sci.* 2010, 86:588-610.
57. Cooper CS, Park M, Blair DG, et al.: Molecular cloning of a new transforming gene from a chemically transformed human cell line. *Nature.* 1984, 311:29-33.
58. Organ SL, Tsao MS: An overview of the c-MET signaling pathway. *Ther Adv Med Oncol.* 2011, 3:S7-S19.
59. Trusolino L, Bertotti A, Comoglio PM: MET signalling: principles and functions in development, organ regeneration and cancer. *Nat Rev Mol Cell Biol.* 2010, 11:834-848.
60. Kermorgant S, Parker PJ: c-Met signalling: spatio-temporal decisions. *Cell Cycle.* 2005, 4:352-355.
61. Jeffers M, Taylor GA, Weidner KM, Omura S, Vande Woude GF: Degradation of the Met tyrosine kinase receptor by the ubiquitin-proteasome pathway. *Mol Cell Biol.* 1997, 17:799-808.
62. Hammond DE, Carter S, McCullough J, et al.: Endosomal dynamics of Met determine signaling output. *Mol Biol Cell.* 2003, 14:1346-1354.

63. Platta HW, Stenmark H: Endocytosis and signaling. *Curr Opin Cell Biol.* 2011, 23:393-403.
64. Prat M, Crepaldi T, Gandino L, et al.: C-terminal truncated forms of Met, the hepatocyte growth factor receptor. *Mol Cell Biol.* 1991, 11:5954-5962.
65. Lee CC, Yamada KM: Identification of a novel type of alternative splicing of a tyrosine kinase receptor. Juxtaposition deletion of the c-met protein kinase C serine phosphorylation regulatory site. *J Biol Chem.* 1994, 269:19457-19461.
66. Gherardi E, Birchmeier W, Birchmeier C, Vande Woude G: Targeting MET in cancer: rationale and progress. *Nat Rev Cancer.* 2012, 12:89-103.
67. Syed ZA, Yin W, Hughes K, et al.: HGF/c-met/Stat3 signaling during skin tumor cell invasion: indications for a positive feedback loop. *BMC Cancer.* 2011, 11:180.
68. Boccaccio C, Ando M, Tamagnone L, et al.: Induction of epithelial tubules by growth factor HGF depends on the STAT pathway. *Nature.* 1998, 391:285-288.
69. Orian-Rousseau V, Morrison H, Matzke A, et al.: Hepatocyte growth factor-induced Ras activation requires ERM proteins linked to both CD44v6 and F-actin. *Mol Biol Cell.* 2007, 18:76-83.
70. Jo M, Stolz DB, Esplen JE, et al.: Cross-talk between epidermal growth factor receptor and c-Met signal pathways in transformed cells. *J Biol Chem.* 2000, 275:8806-8811.
71. Owusu BY, Galemno R, Janetka J, Klampfer L: Hepatocyte Growth Factor, a Key Tumor-Promoting Factor in the Tumor Microenvironment. *Cancers (Basel).* 2017, 9.
72. Lee C, Whang YM, Campbell P, et al.: Dual targeting c-met and VEGFR2 in osteoblasts suppresses growth and osteolysis of prostate cancer bone metastasis. *Cancer Lett.* 2018, 414:205-213.
73. Ricci G, Catizone A, Innocenzi A, Galdieri M: Hepatocyte growth factor (HGF) receptor expression and role of HGF during

- embryonic mouse testis development. *Dev Biol.* 1999, 216:340-347.
74. Ricci G, Catizone A, Galdieri M: Pleiotropic activity of hepatocyte growth factor during embryonic mouse testis development. *Mech Dev.* 2002, 118:19-28.
75. Ricci G, Catizone A: Pleiotropic Activities of HGF/c-Met System in Testicular Physiology: Paracrine and Endocrine Implications. *Front Endocrinol (Lausanne).* 2014, 5:38.
76. Ricci G, Catizone A, Galdieri M: Expression and functional role of hepatocyte growth factor and its receptor (c-met) during fetal mouse testis development. *J Endocrinol.* 2006, 191:559-570.
77. Ricci G, Guglielmo MC, Caruso M, et al.: Hepatocyte growth factor is a mouse fetal Leydig cell terminal differentiation factor. *Biol Reprod.* 2012, 87:146.
78. Catizone A, Ricci G, Galdieri M: Functional role of hepatocyte growth factor receptor during sperm maturation. *J Androl.* 2002, 23:911-918.
79. Catizone A, Ricci G, Arista V, Innocenzi A, Galdieri M: Hepatocyte growth factor and c-MET are expressed in rat prepubertal testis. *Endocrinology.* 1999, 140:3106-3113.
80. Catizone A, Ricci G, Galdieri M: Expression and functional role of hepatocyte growth factor receptor (C-MET) during postnatal rat testis development. *Endocrinology.* 2001, 142:1828-1834.
81. Del Bravo J, Catizone A, Ricci G, Galdieri M: Hepatocyte growth factor-modulated rat Leydig cell functions. *J Androl.* 2007, 28:866-874.
82. Catizone A, Ricci G, Caruso M, et al.: Hepatocyte growth factor (HGF) regulates blood-testis barrier (BTB) in adult rats. *Mol Cell Endocrinol.* 2012, 348:135-146.
83. Depuydt CE, Zalata A, de Potter CR, van Emmelo J, Comhaire FH: The receptor encoded by the human C-MET oncogene is expressed in testicular tissue and on human spermatozoa. *Mol Hum Reprod.* 1996, 2:2-8.

84. Depuydt CE, De Potter CR, Zalata A, et al.: Levels of hepatocyte growth factor/scatter factor (HGF/SF) in seminal plasma of patients with andrological diseases. *J Androl.* 1998, *19*:175-182.
85. Garajova I, Giovannetti E, Biasco G, Peters GJ: c-Met as a Target for Personalized Therapy. *Transl Oncogenomics.* 2015, *7*:13-31.
86. Olivero M, Valente G, Bardelli A, et al.: Novel mutation in the ATP-binding site of the MET oncogene tyrosine kinase in a HPRCC family. *Int J Cancer.* 1999, *82*:640-643.
87. Lubensky IA, Schmidt L, Zhuang Z, et al.: Hereditary and sporadic papillary renal carcinomas with c-met mutations share a distinct morphological phenotype. *Am J Pathol.* 1999, *155*:517-526.
88. Park WS, Dong SM, Kim SY, et al.: Somatic mutations in the kinase domain of the Met/hepatocyte growth factor receptor gene in childhood hepatocellular carcinomas. *Cancer Res.* 1999, *59*:307-310.
89. Lorenzato A, Olivero M, Patane S, et al.: Novel somatic mutations of the MET oncogene in human carcinoma metastases activating cell motility and invasion. *Cancer Res.* 2002, *62*:7025-7030.
90. Matsumoto K, Nakamura T: Hepatocyte growth factor and the Met system as a mediator of tumor-stromal interactions. *Int J Cancer.* 2006, *119*:477-483.
91. Koeppen H, Rost S, Yauch RL: Developing biomarkers to predict benefit from HGF/MET pathway inhibitors. *J Pathol.* 2014, *232*:210-218.
92. Eder JP, Vande Woude GF, Boerner SA, LoRusso PM: Novel therapeutic inhibitors of the c-Met signaling pathway in cancer. *Clin Cancer Res.* 2009, *15*:2207-2214.
93. Parikh RA, Wang P, Beumer JH, Chu E, Appleman LJ: The potential roles of hepatocyte growth factor (HGF)-MET pathway inhibitors in cancer treatment. *Onco Targets Ther.* 2014, *7*:969-983.

94. Engelman JA, Zejnullahu K, Mitsudomi T, et al.: MET amplification leads to gefitinib resistance in lung cancer by activating ERBB3 signaling. *Science*. 2007, *316*:1039-1043.
95. Bardelli A, Corso S, Bertotti A, et al.: Amplification of the MET receptor drives resistance to anti-EGFR therapies in colorectal cancer. *Cancer Discov*. 2013, *3*:658-673.
96. Song N, Liu S, Zhang J, et al.: Cetuximab-induced MET activation acts as a novel resistance mechanism in colon cancer cells. *Int J Mol Sci*. 2014, *15*:5838-5851.
97. Cascone T, Xu L, Lin HY, et al.: The HGF/c-MET Pathway Is a Driver and Biomarker of VEGFR-inhibitor Resistance and Vascular Remodeling in Non-Small Cell Lung Cancer. *Clin Cancer Res*. 2017, *23*:5489-5501.
98. Apicella M, Giannoni E, Fiore S, et al.: Increased Lactate Secretion by Cancer Cells Sustains Non-cell-autonomous Adaptive Resistance to MET and EGFR Targeted Therapies. *Cell Metab*. 2018, *28*:848-865 e846.
99. Mostert MM, van de Pol M, Olde Weghuis D, et al.: Comparative genomic hybridization of germ cell tumors of the adult testis: confirmation of karyotypic findings and identification of a 12p-amplicon. *Cancer Genet Cytogenet*. 1996, *89*:146-152.
100. Kawakami T, Okamoto K, Sugihara H, et al.: The MET proto-oncogene is not a major target for the gain of chromosome 7 in testicular germ-cell tumors of adolescents. *Virchows Arch*. 2004, *444*:480-481.
101. Svetlovska D, Miskovska V, Cholujova D, et al.: Plasma Cytokines Correlated With Disease Characteristics, Progression-Free Survival, and Overall Survival in Testicular Germ-Cell Tumor Patients. *Clin Genitourin Cancer*. 2017, *15*:411-416 e412.
102. Scheri KC, Leonetti E, Laino L, et al.: c-MET receptor as potential biomarker and target molecule for malignant testicular germ cell tumors. *Oncotarget*. 2018, *9*:31842-31860.
103. Leonetti E, Gesualdi L, Scheri KC, et al.: c-Src Recruitment is Involved in c-MET-Mediated Malignant Behaviour of NT2D1 Non-Seminoma Cells. *Int J Mol Sci*. 2019, *20*.

104. Takahashi A, Obata Y, Fukumoto Y, et al.: Nuclear localization of Src-family tyrosine kinases is required for growth factor-induced euchromatinization. *Exp Cell Res.* 2009, *315*:1117-1141.
105. Paladino D, Yue P, Furuya H, et al.: A novel nuclear Src and p300 signaling axis controls migratory and invasive behavior in pancreatic cancer. *Oncotarget.* 2016, *7*:7253-7267.
106. Urciuoli E, Coletta I, Rizzuto E, et al.: Src nuclear localization and its prognostic relevance in human osteosarcoma. *J Cell Physiol.* 2018, *233*:1658-1670.
107. Birchmeier C, Birchmeier W, Gherardi E, Vande Woude GF: Met, metastasis, motility and more. *Nat Rev Mol Cell Biol.* 2003, *4*:915-925.
108. Zafarana G, Grygalewicz B, Gillis AJ, et al.: 12p-amplicon structure analysis in testicular germ cell tumors of adolescents and adults by array CGH. *Oncogene.* 2003, *22*:7695-7701.
109. Shen H, Shih J, Hollern DP, et al.: Integrated Molecular Characterization of Testicular Germ Cell Tumors. *Cell Rep.* 2018, *23*:3392-3406.

Erica Leonetti

Pag 98

List of publications

Leonetti Erica, Gesualdi Luisa, Corano Scheri Katia, Dinicola Simona, Fattore Luigi, Masiello Maria Grazia, Cucina Alessandra, Mancini Rita, Bizzarri Mariano, Ricci Giulia, Catizone Angela (2019). c-Src recruitment is Involved in c-MET-mediated malignant behaviour of NT2D1 non-seminoma cells. INTERNATIONAL JOURNAL OF MOLECULAR SCIENCES, vol. 20, p. 1- 21, ISSN: 1422-0067, doi: 10.3390/ijms20020320.

Proietti Sara, Cucina Alessandra, Pensotti Andrea, Biava Pier Mario, Minini Mirko, Monti Noemi, Catizone Angela, Ricci Giulia, Leonetti Erica, Harrath Abdel Halim, Alwasel Saleh H, Bizzarri Mariano (2019). Active fraction from embryo fish extracts induces reversion of the malignant invasive phenotype in breast cancer through down-regulation of TCTP and modulation of E-cadherin/ β -catenin pathway. INTERNATIONAL JOURNAL OF MOLECULAR SCIENCES, vol. 20, ISSN: 1422-0067, doi: 10.3390/ijms20092151.

Corano Scheri K, Leonetti E, Laino L, Gigantino V, Gesualdi L, Grammatico P, Bizzari M, Franco R, Oosterhuis JW, Stoop H, Looijenga LHJ, Ricci G, Catizone A. (2018). c-MET receptor as potential biomarker and target molecule for malignant testicular germ cell tumors. ONCOTARGET, vol. 9, p. 31842-31860, ISSN: 1949-2553, doi: 10.18632/oncotarget.25867.

Erica Leonetti

Congress communications

Erica Leonetti, Luisa Gesualdi, Luigi Fattore, Marcella Cammarota, Chiara Schiraldi, Mariano Bizzarri, Bianca Maria Scicchitano, Alessandra Cucina, Rita Mancini, Angela Catizone, Giulia Ricci. PI3K/AKT role in the c-Met-mediated malignant behaviour of NT2D1 non- seminoma cells.

4° Annual Meeting ACC; 20-22 November 2019, Rome, Italy.

Luisa Gesualdi, E. Leonetti, B.M. Scicchitano, S. Sorrentino, A. Barbiera, L. Fattore, R. Mancini, G. Ricci, A. Catizone. ERK role in the c-MET-mediated proliferating behaviour of NT2D1 non-seminoma cells.

4° Annual Meeting ACC; 20-22 November 2019, Rome, Italy.

Erica Leonetti, Luisa Gesualdi, Luigi Fattore, Marcella Cammarota, Chiara Schiraldi, Mariano Bizzarri, Bianca Maria Scicchitano, Alessandra Cucina, Rita Mancini, Angela Catizone, Giulia Ricci. PI3K/AKT role in the c-Met-mediated malignant behaviour of NT2D1 non- seminoma cells.

SIAI, 73° National Congress, 22-24 September 2019, Napoli, Italy.

Erica Leonetti, Luisa Gesualdi, Luigi Fattore, Marcella Cammarota, Chiara Schiraldi, Mariano Bizzarri, Bianca Maria Scicchitano, Alessandra Cucina, Rita Mancini, Angela Catizone, Giulia Ricci. c-Met-mediated pathway in malignant behaviour acquisition of NT2D1 non- seminoma cells: role of PI3K/AKT and c-Src adaptors.

ABCD National Congress; 19-21 September 2019, Bologna, Italy.

Luisa Gesualdi, E. Leonetti, B.M. Scicchitano, S. Sorrentino, A. Barbiera, L. Fattore, R. Mancini, G. Ricci, A. Catizone. ERK role in the c-MET-mediated proliferating behaviour of NT2D1 non-seminoma cells.

ABCD National Congress; 19-21 September 2019, Bologna, Italy.

Erica Leonetti

Leonetti Erica, Gesualdi Luisa, Corano Scheri Katia, Dinicola Simona, Fattore Luigi, Masiello Maria Grazia, Cucina Alessandra, Mancini Rita, Bizzarri Mariano, Ricci Giulia, Catizone Angela. c-Src Recruitment is Involved in c-MET-Mediated Malignant Behaviour of NT2D1 Non-Seminoma Cells.

Speaker during: College of histology and embriology professors, February 22th 2019.

Erica Leonetti, Luisa Gesualdi, Simona Dinicola, Maria Grazia Masiello, Mariano Bizzarri, Alessandra Cucina, Angela Catizone, Giulia Ricci. PI3K role in the c-Met-mediated migrating and invading behavior of NT2D1 non-seminoma cells.

XV FISV Congress, 18-21 September 2018, Sapienza University of Rome.

Leonetti E., Gesualdi L., Dinicola S., Masiello M. G., Bizzarri M., Cucina A., Catizone A., Ricci G. c-Src is involved in the c-MET-mediated migrating and invading behavior of NT2D1 Embryonal Carcinoma cells.

10th European Congress of Andrology, October 11-13, 2018, Budapest, Hungary.

Corano Scheri Katia, Ricci, Giulia, Leonetti, Erica, Gesualdi, L., Oosterhuis, J. W., Stoop, J., Looijenga, A. Catizone, L. H. J. c-MET receptor: a potential biomarker for Testicular Germ Cell Tumours.

10th NYRA meeting, 11-13 September 2017, Brussels, Belgium.

Erica Leonetti, Katia Corano Scheri, Luisa Gesualdi, Marcella Cammarota, Chiara Schiraldi, Mariano Bizzarri, Angela Catizone, Giulia Ricci. Microgravity promotes gap junctional contact formation in TCam-2 seminoma cells grown in low adhesion as embryoid bodies.

ABCD National Congress; 21-23 September 2017, Bologna, Italy.

Corano Scheri, Katia, Leonetti, Erica, Gesualdi, L., Ricci, G., Catizone, Angiolina. HGF/c-Met pathway in seminoma and non-seminoma cell lines: role in cell invasion.

VII BeMM Symposium. Rome, Italy, 18 November 2016.

Erica Leonetti

Acknowledgments

La fine di ogni percorso porta con sé tutta una serie di sentimenti contrastanti: gioia, malinconia, tristezza, rimpianti...

E con oggi, un capitolo importante della mia vita si conclude, un capitolo fatto di alti e bassi, sacrifici e gioie, amarezza ed infinita soddisfazione.

Ma nulla sarebbe stato lo stesso senza le persone che mi sono state costantemente accanto durante tutte le tappe che hanno caratterizzato questa avventura. Le mie certezze.

Un primo e doveroso ringraziamento va a tutta la sezione di istologia ed embriologia del dipartimento SAIMLAL, diventata ormai, a tutti gli effetti, una seconda casa. Ringrazio inoltre il coordinatore del corso del dottorato, il professore Antonio Musarò, per essere un punto di riferimento per tutti noi studenti.

Ma in particolare, desidero ringraziare le mie tutor, Giulia ed Angela, che con il loro impegno ed il tempo dedicato mi hanno permesso di portare avanti il mio progetto. La vostra saggezza, la fiducia e l'affetto dimostratomi mi hanno guidato verso una crescita professionale e personale per le quali vi sarò sempre grata.

Un grazie di cuore va a tutte le mie amiche/colleghe, che nel tempo sono diventate per me la mia famiglia romana.

Grazie alla mia compagna di avventure nel laboratorio 25, la mia piccola Luisa, senza di te nulla sarebbe stato lo stesso in questi anni. Mi hai aiutato ad affrontare ogni momento di sconforto e sei stata al mio fianco in ogni mia vittoria.

In questo periodo ho avuto la fortuna di incontrare sulla mia strada persone meravigliose. Al di là della porta di legno del lab25, bastava fare qualche passo nel corridoio per trovare supporto e coraggio in quelle che ormai sono diventate figure essenziali nella mia vita: Ernestina, la mia dolce metà, la spalla su cui più volte ho pianto, amica e compagna di risate. La piccola e dolce Claudia, amica fidata e confidente preziosa. Rita, una delle persone più

buone e pure che io abbia mai conosciuto. Annina dolce, pronta a contagiare tutti con il suo ottimismo. Jairo, dispensatore di sorrisi, gioia e buon umore. Rosanna & Piera, compagne di bevute inarrivabili! Grazie anche a Saretta per tutte le volte che con un semplice cioccolatino è riuscita a strapparmi un sorriso, ed alla saggia Stefania De Grossi, i cui consigli sono scolpiti indelebili nella mia testa. E grazie anche a voi, Federica Campolo e Barbagallo, per non esservi mai tirate indietro dal tendermi una mano, con gentilezza e disponibilità, ogni qual volta ho avuto bisogno di voi.

Un ringraziamento speciale va senza dubbio alla mia meravigliosa e complicata famiglia. Alla mia mamma ed al mio papà, che mai hanno smesso di credere in me. Mi hanno fornito, seppure a distanza, tutto il loro supporto ed amore incondizionati, mai mutati nel corso dei miei 31 anni.

Alle mie super zie, Concetta e Stefania, da sempre per me “porto sicuro” ricco di amore.

A Giorgia e Laura che mi hanno fatto capire cosa volesse dire amore assoluto.

Grazie alla mia famiglia ritrovata, a zio Roberto ed al sincero affetto che nutre nei miei confronti.

Alle mie cugine, tutte. Ma un grazie particolare a Silvia, al mio fianco da una vita intera.

Ma non solo. Se è vero che in questi anni ho capito che per essere una Famiglia non basta condividere parte del proprio patrimonio genetico, ma è fondamentale amarsi e rispettarsi, sempre, nella gioia e, ancor di più, nel dolore... grazie alla Famiglia meravigliosa su cui so di poter sempre contare!

Grazie alla mia Barbara, amica leale e sincera, mia roccia e fonte di energia.

Un enorme e gigantesco GRAZIE lo merita colui che mi ha appoggiato e sostenuto in ogni momento. Colui che ha sopportato

tutto il “peggio” che è venuto fuori in questi ultimi anni: le mie lacrime, la mia rabbia e la mia insicurezza. Senza Francesco, che mi ha amorevolmente accompagnata in questo tragitto, sicuramente non sarei riuscita a superare neanche il primo mese di questa avventura!

Un ringraziamento speciale poi a te che sei la mia persona, la mia confidente, amica, sorella, complice, l'altra metà della mia mela. A te, Federica, dico sinceramente grazie. Grazie perché con il tuo affetto sei riuscita a superare ogni distanza, grazie per la tua capacità di capirmi al volo in ogni situazione, grazie per essere l'amica perfetta che tutti vorrebbero avere, per essere come sei e non deludermi mai, grazie per essere diventata parte integrante della mia famiglia e per farmi sentire casa ogni posto in cui sei tu. Grazie semplicemente per ESSERCI.

Ed infine, ma non per importanza, un sentito GRAZIE a me, per aver trovato sempre il coraggio e la forza di rialzarmi dopo ogni caduta, per non essermi mai arresa e per aver affrontato ogni situazione sempre a testa alta. Forse, dopo tanto tempo, ho capito davvero quanto valgo.